

**AIR WATER LOOP-  
AN EXPERIMENTAL FACILITY TO STUDY THERMAL  
HYDRAULICS OF AHWR STEAM DRUM**

by

**R.K. Bagul, D.S. Pilkhwal, V. Jain and P.K. Vijayan**  
Reactor Engineering Division

GOVERNMENT OF INDIA  
ATOMIC ENERGY COMMISSION

**AIR WATER LOOP-  
AN EXPERIMENTAL FACILITY TO STUDY THERMAL  
HYDRAULICS OF AHWR STEAM DRUM**

by

**R.K. Bagul, D.S. Pilkhwal, V. Jain and P.K. Vijayan**  
Reactor Engineering Division

BHABHA ATOMIC RESEARCH CENTRE  
MUMBAI, INDIA  
2014

**BIBLIOGRAPHIC DESCRIPTION SHEET FOR TECHNICAL REPORT**  
(as per IS : 9400 - 1980)

01	<i>Security classification :</i>	Unclassified
02	<i>Distribution :</i>	External
03	<i>Report status :</i>	New
04	<i>Series :</i>	BARC External
05	<i>Report type :</i>	Technical Report
06	<i>Report No. :</i>	BARC/2014/E/001
07	<i>Part No. or Volume No. :</i>	
08	<i>Contract No. :</i>	
10	<i>Title and subtitle :</i>	Air water loop - an experimental facility to study thermal hydraulics of AHWR steam drum
11	<i>Collation :</i>	55 p., 17 figs., 4 tabs., 2 ill.
13	<i>Project No. :</i>	
20	<i>Personal author(s) :</i>	R.K. Bagul; D.S. Pilkhwal; V. Jain; P.K. Vijayan
21	<i>Affiliation of author(s) :</i>	Reactor Engineering Division, Bhabha Atomic Research Centre, Mumbai
22	<i>Corporate author(s) :</i>	Bhabha Atomic Research Centre, Mumbai - 400 085
23	<i>Originating unit :</i>	Reactor Engineering Division, Bhabha Atomic Research Centre, Mumbai
24	<i>Sponsor(s) Name :</i>	Department of Atomic Energy
	<i>Type :</i>	Government

Contd...

30	<i>Date of submission :</i>	April 2014
31	<i>Publication/Issue date :</i>	May 2014
40	<i>Publisher/Distributor :</i>	Head, Scientific Information Resource Division, Bhabha Atomic Research Centre, Mumbai
42	<i>Form of distribution :</i>	Hard copy
50	<i>Language of text :</i>	English
51	<i>Language of summary :</i>	English, Hindi
52	<i>No. of references :</i>	7 refs.
53	<i>Gives data on :</i>	
60	<i>Abstract :</i>	In the proposed Indian Advanced Heavy Water Reactor (AHWR) the coolant re-circulation in the primary system is achieved by two-phase natural circulation. The two-phase steam-water mixture from the reactor core is separated in steam drum by gravity. Gravity separation of phases may lead to undesirable phenomena – carryover and carryunder. Carryover is the entrainment of liquid droplets in the vapor phase. Carryover needs to be minimized to avoid erosion corrosion of turbine blades. Carryunder is the entrainment of vapor bubbles with liquid flowing back to reactor core. Significant carryunder may in turn lead to reduced flow resulting in reduced CHF margin and stability in the coolant channel. An Air-Water Loop (AWL) has been designed to carry out the experiments relevant to AHWR steam drum. The design features and scaling philosophy is described in this report
70	<i>Keywords/Descriptors :</i>	HWLWR TYPE REACTORS; PRIMARY COOLANT CIRCUITS; REACTOR CORES; TURBINE BLADES; DESIGN; THERMAL HYDRAULICS
71	<i>INIS Subject Category :</i>	S21
99	<i>Supplementary elements :</i>	

## ***Abstract***

*In the proposed Indian Advanced Heavy Water Reactor (AHWR) the coolant recirculation in the primary system is achieved by two-phase natural circulation. The two-phase steam-water mixture from the reactor core is separated in steam drum by gravity. Gravity separation of phases may lead to undesirable phenomena – carryover and carryunder. Carryover is the entrainment of liquid droplets in the vapor phase. Carryover needs to be minimized to avoid erosion corrosion of turbine blades. Carryunder is the entrainment of vapor bubbles with liquid flowing back to reactor core. Significant carryunder may in turn lead to reduced flow resulting in reduced CHF margin and stability in the coolant channel.*

*An Air-Water Loop (AWL) has been designed to carry out the experiments relevant to AHWR steam drum. The design features and scaling philosophy is described in this report.*

## सारांश

प्रस्तावित भारतीय उन्नत भारी जल रिएक्टर (AHWR) के प्राथमिक प्रणाली में शितलक का प्रचलन द्वि-स्थितीय प्राकृतिक संचलन द्वारा हासिल किया गया है। रिएक्टर कोर से निकलने वाला द्वि-स्थितीय भाप-पानी का मिश्रण भाप पीपा (drum) में गुरुत्वाकर्षण द्वारा पृथक होता है। गुरुत्वाकर्षण द्वारा किया जाने वाला पृथक्करण carryover और carryunder जैसे आपत्तिजनक स्थितियों को जन्म दे सकती है। carryover पानी के बूंदों का भाप के साथ वहन होना है। Carryover टर्बाइन ब्लेड के कटाव / जंग से बचने के लिए कम किया जाना चाहिए। carryunder वाष्प के बुलबुलो का पानी के साथ रिएक्टर कोर में वहन होना है। Carryunder के ज्यादा मात्रा से प्राकृतिक संचलन प्रवाह कम होकर परिणामस्वरूप CHF मार्जिन तथा प्रवाह स्थिरता प्रभावित होती है।

Carryover और carryunder का अध्ययन करने तथा AHWR भाप पीपा संबंधित प्रयोग करने हेतु Air-Water Loop (AWL) का अभिकल्पन किया गया है। यह रिपोर्ट AWL के अभिकल्पन विशेषताओं को और अनुमाप परिवर्तन सिद्धांतों का विवरण प्रस्तुत करता है।

## CONTENTS

1.0	Introduction	1
2.0	Objectives of AWL	3
3.0	Brief Description of AHWR primary loop	3
4.0	Steam drum of AHWR	4
5.0	Salient features of AWL	5
6.0	Scaling Methodology	5
7.0	Applicability of scaling to latest design of steam drum	6
8.0	Experimental programs	10
9.0	Instrumentation and parameters to be measured	10
10.0	Pre-test analysis	11
10.1	Steady state flow analysis	11
10.2	Carryover analysis	12
10.3	Carryunder analysis	15
11.0	Results and Discussions	16
12.0	Concluding Remarks	17
	Nomenclature	18
	References	19
	Appendix-A	21
	Appendix-B	29

## **List of Figures**

Fig. 1: Schematic of PHT system of AHWR

Fig. 2a: Prototype steam drum (previous version)

Fig. 2b: AHWR steam drum (latest revised version)

Fig. 3: Schematic of Air Water Loop

Fig. 4: Isometric view of Air Water Loop

Fig. 5: Air water drum and Water tank

Fig. 6: Air injection Header and Air injection lines.

Fig. 7: Tail pipes and Air injection lines.

Fig. 8: Nodalisation used for pre-test steady state flow analysis

Fig. 9: Air flow rate variation with void fraction

Fig. 10: Variation of water flow rate with void fraction

Fig. 11: Variation of void fraction in tail pipe, steam drum riser and steam drum pool

Fig. 12: Comparison of void fraction in tail pipe

Fig. 13: Comparison of void fraction in steam drum riser

Fig. 14: Comparison of void fraction at steam water interface

Fig. 15: Comparison of maximum droplet and critical diameter for model and prototype steam drum

Fig. 16: Effect of air velocity on carryover for model and prototype steam drum

Fig. 17: Effect of air velocity on carryunder for model and prototype steam drum



## **List of tables**

Table 1: Parameters for scaling the AHWR steam drum

Table-2: Comparison of different dimensions of prototype and Model SD

Table-3: Comparison of scaling parameters for prototype and model.

Table 4: Sizing of different components of AWL

## **List of appendices**

APPENDIX-A: SIZING OF VARIOUS COMPONENTS OF AWL

APPENDIX-B: Applicability of AWL scaling to the latest design of AHWR steam drum

## 1.0 Introduction

The proposed Indian Advanced Heavy Water (AHWR) which is under advanced stage of design is a heavy water moderated, boiling light water cooled pressure tube type reactor. The coolant recirculation in the primary system is achieved by two-phase natural circulation, which depends on the density difference between the hot and cold legs of the primary loop. The two-phase steam-water mixture leaving the core of the reactor enters the steam drum through tail pipes. The steam-water separation is achieved in AHWR steam drum naturally without the use of a mechanical separator. Free surface gravity separation is employed for steam-water separation in the steam drum. The steam flows to the turbine and separated water is mixed with the subcooled feed water at the bottom of steam drum and flows to the reactor core through downcomer and feeders.

Steam-water separation without the aid of mechanical separators may not be effective for complete separation and may lead to two undesirable phenomena i.e. carryover and carryunder. Both these phenomena are essentially the entrainment of one phase by another, and are typical of equipment where the relative motion between two phases is encountered.

Carryover is the entrainment of liquid droplets in the vapor phase. Some amount of water in the form of small droplets may be carried over with steam to the turbine circuit, if the separation of steam-water in the steam drum is not complete. Carryover should be eliminated as much as possible to avoid erosion corrosion of the turbine blades. The carryover depends on the geometrical parameters of the steam drum like diameter, height available for separation along with the operating conditions like pressure and steam velocity.

Carryunder is the entrainment of gas bubbles along with the liquid flowing from steam drum to the downcomer. It is particularly undesirable in a natural circulation system, where the driving force for the flow is caused by the density difference between hot and cold legs. Significant carryunder may in turn lead to reduced CHF margin in the coolant channel. The carryunder phenomenon depends on the steam drum diameter, baffle height and baffle spacing as well as operating conditions such as pressure, feed water temperature and downcomer velocity.

Computer codes GSEP-CO for carryover<sup>1</sup> and GSEP-CU for carryunder<sup>2</sup> have been developed in-house which use correlations for pool entrainment, droplet size distribution and bubble size distribution in the steam drum. These codes need to be validated against experimental data.

In the normal operating conditions of the reactor the average core exit quality is about 19.1% which corresponds to a void fraction of 82.79%. This causes a swelling in the steam drum (i.e. an increase in the steam drum level). The void fraction correlations for the small diameter pipes (Such as tail pipes) are available which are validated but for the large diameter pipe or pool (such as steam drum) such correlations are not available. In the case of reactor trip the water level in the steam drum will fall due to collapse of voids. Therefore, studies are required to know the exact void fraction and swelling in the steam drum. In view of this, the measurement will be carried out for the pool void fraction and swelling in the steam drum of AWL in order to develop the correlations for the void fraction in the pool.

Model testing in a reasonably large scale facility using steam-water flow is ruled out because of the enormous cost involved. Under these circumstances it was decided to carry out experiments in a small scale steam drum using air-water flow to generate the above mentioned empirical inputs.

In view of the above an Air Water Loop (AWL) has been designed, fabricated, installed and commissioned to carry out the experiments relevant to Advanced Heavy Water Reactors (AHWR). The steam drum has been scaled down by keeping the superficial velocities same at different regions of the steam drum. Calculations of steady state flow for the AWL has been carried out for different air flow rates to check the adequacy of the model design. The carryover and carryunder analyses have been also carried out using above mentioned codes for the model as well as the prototype steam drum with air water.

The objectives, preliminary design features of this loop, results of the steady state analysis and the results of the carryunder analyses are described in this report.

## 2.0 Objectives of Air-Water Loop

An AWL has been designed in BARC. This loop will be used to cater to following objectives;

- Investigation of the carryover and carryunder phenomenon in steam drum of AHWR,
- To measure the swell in the steam drum,
- To test performance of various steam drum internals i.e. vortex breaker and slug breaker plate.

## 3.0 Brief description of AHWR primary loop

AHWR is a natural circulation based nuclear reactor, where the primary flow is due to the difference in densities of the coolant in the hot and cold legs of the primary loop. This difference in densities gives rise to a buoyancy force. When the buoyancy force generated is balanced by retarding friction forces, the primary flow attains a steady state. The AHWR primary loop consists of a common reactor inlet header (RIH) from which 452 inlet feeders branch out to an equal number of fuel channels in the vertical core. The outlets from these fuel channels are connected to equal number of tail pipes. There are four steam drums. Each steam drum is connected to 113 tail pipes. From each steam drum, four downcomer pipes are connected to common inlet header. Fig. 1 illustrates the schematic of the main PHT system with the relative elevation of the various components and their sizes.

During normal operating conditions the steam drum pressure is maintained at 7 MPa. The level of water in the steam drum at nominal operating conditions is 2.2 m. The two-phase mixture leaving the core is separated into steam and water in the steam drum. The steam water separation in AHWR steam drum is achieved naturally by gravity separation without the use of mechanical separators. At the normal operating condition about 408 kg/s of steam, separated in the steam drums, flows into the turbine and an equal mass rate of feed water enters the steam drum at 130<sup>o</sup> C. The outlet temperature of the water from the steam drum is about 261.4<sup>o</sup> C at nominal operating conditions assuming the complete mixing of feed water with saturated water in the steam drum. The primary loop circulation rate maintained by the density difference is

approximately 2141 kg/s at nominal operating condition. The average core exit quality is about 19.1 % for the rated reactor operating condition.

#### **4.0 Steam drum of AHWR.**

Since the inception of concept of AHWR, steam drum design has been updated at various stages. Fig. 2a shows the configuration of AHWR steam drum at the time of design of AWL which is a cylindrical vessel (3.75 m ID, 11 m length) closed at both the ends by torispherical heads. The two phase steam water mixture produced in the core enters each of four identical steam drums through tail pipes connected to the coolant channels. Longitudinal partition plates provided inside each steam drum prevents the mixing of the incoming steam with the subcooled feed water. The height of the partition plates is such that it remains submerged with water at zero power hot shut down condition. Steam is taken out from each steam drum through single steam outlet nozzle located at the top of the steam drum. The experimental facility AWL has been designed according to this version of steam drum available at that time.

Fig. 2b shows the latest configuration of AHWR steam drum. It is a horizontal pressure vessel with cylindrical cross-sectional closed at the ends with torispherical dish heads. The internal diameter of steam drum is 4.0 m and total length of vessel is 11.0 m. There are 4 downcomers (300 NB Sch. 120 pipe) provided at the bottom centre of steam drum. 113 tail pipes enter into steam drum from both sides of the downcomer at different angles as shown in Fig. 2b. Longitudinal baffle plates are provided to prevent the two-phase mixture from tail-pipe to enter in downcomer region. Lower submerged perforated plate is provided at the top of baffle plate, which breaks down large slug bubbles coming from tailpipe into smaller bubbles. This shall reduce the fluctuations of the separation interface. Upper submerged perforated plate is provided in steam drum pool region just above the centerline. This plate distributes the bubbles in the pool and thus functions to reduce the turbulence of the free surface at separation interface. Overhead perforated plate offers additional resistance to the steam flow and minimizes the droplets entraining in the steam flow. There are four nozzles and piping (200 NB Sch. 120) provided for steam collection into the steam collector header (300 NB Sch. 120). Steam is sent from collection header to the turbine for power production.

Following sections describe the salient features, scaling methodology for this prototype model version (3.75 m ID, 11 m length). A section will also address the applicability of the design to the latest version of the steam drum design.

## **5.0 Salient features of AWL**

A multi-channel air-water loop (AWL) has been designed and fabricated. Fig. 3 shows the schematic of the AWL. It consists of an air-water drum, tail pipes, down comers, storage tank, air injection lines, air separation line. The air-water drum simulates 1/8th slice of the prototype (with a volume scaling of 1:10), with 14 tail pipes (62.7 mm ID) and one downcomer (97.15 mm ID). The air-water drum is fabricated with 15 tailpipe connections, one of which can be blocked to simulate 14 tailpipes. One end of these tail pipes and downcomer is connected to the air-water drum as in the prototype while other end is connected to a storage tank. The air-water drum has three plane surfaces and one SS curved surface. The two plane adjoining sides are made of transparent and the curved and third plane side is made of SS. Air is injected at the bottom end of the vertical tail pipes. Due to the driving force provided by the density difference a circulation is established in the loop. The two-phase flow of air-water mixture then enters the vertical test section and passes through the steam drum riser and finally to the separator drum. Traces of water in the air are separated through a separator, which is open to the atmosphere as shown in the schematic diagram. The total loop occupies a space of 4 m x 7 m x 8 m (floor area × height) with a design pressure of 2 bar. Loop flow is generated by natural circulation – density difference between single-phase water and two-phase air-water mixture. Fig. 4 shows the isometric view of the experimental loop. Fig.s 5 to 7 show photographs of the facility and its components.

## **6.0 Scaling methodology**

As stated earlier, the primary objective of the AWL is to investigate the carryover and carryunder phenomenon relevant to AHWR along with the pool swelling phenomenon in the steam drum. The scaling of the steam drum has been given primary importance. From the description of the prototype steam drum it appears that if torispherical heads are not considered, the locations of

tail pipes and downcomers have a  $1/4^{\text{th}}$  symmetry. Therefore for full scale simulation it is only required to simulate  $1/4^{\text{th}}$  of steam drum with a single downcomer and 28 tail pipes. This requires an air flow rate of 41445.0 lpm and a water flow rate of 9546.0 lpm. But the available air flow rate is limited to 16986 lpm in Engineering Hall-7, BARC. Hence it has been modeled in such a way that it can simulate the  $1/8^{\text{th}}$  of a steam drum with 14 tail pipes. The superficial velocities at inlet and outlet of the steam drum have been simulated. The loss coefficients at the inlet and outlet are also simulated.

For proper scaling of the carry-over and carry-under of the steam drum, the different parameters which are preserved are indicated in Table 1.

The detailed calculations are presented in Appendix-A. The different dimensions of the AWL steam drum are compared with that of prototype in Table 2.

### **7.0 Applicability of scaling to latest design of steam drum**

In view of the changes that have been incorporated in the prototype steam drum after the AWL was scaled and designed, the suitability of scaling to the latest available design has been investigated. The scaling parameters as given in Table 1 have been recalculated for prototype design. The detailed calculations are presented in Appendix-B. Table 4 shows the comparison of scaling parameters for model, earlier prototype and latest revision of prototype. The superficial velocities in tail pipe show maximum deviation of 19 %, while the superficial velocities in steam drum regions are within +13.82 to -6.62 %. Ratio of steam drum length to diameter differs from prototype-2 by 22.6 %. Overall scaling distortion with respect to flow variables has been found to be within 20 %.

**Table 1: Parameters for scaling the AHWR steam drum**

<b>Sr. No.</b>	<b>Parameters for scaling</b>	<b>Location in SD</b>
1.	$(J_{G-TP})_P = (J_{G-TP})_M$	Superficial velocity of gas in the tail pipe
2.	$(J_{L-TP})_P = (J_{L-TP})_M$	Superficial velocity of liquid in the tail pipe
3.	$\left(\frac{\text{Tail pipe pitch}}{\text{Tail pipe diameter}}\right)_P = \left(\frac{\text{Tail pipe pitch}}{\text{Tail pipe diameter}}\right)_M$	Ratio of tail pipe pitch and diameter
4.	$(\text{Entry losses})_P = (\text{Entry losses})_M$	In to the steam drum
5.	$(J_{G-R})_P = (J_{G-R})_M$	In the riser at baffle top level
6.	$(J_{L-R})_P = (J_{L-R})_M$	In the riser at baffle top level
7.	$(J_{G-IF})_P = (J_{G-IF})_M$	At interface in the steam drum
8.	$(J_{L-BI})_P = (J_{L-BI})_M$	Horizontal cross flow over the baffle plate
9.	$(J_{L-BS})_P = (J_{L-BS})_M$	In steam drum downcomer region between the longitudinal baffles
10.	$(\text{Local losses at downcomer})_P = (\text{Local losses at downcomer})_M$	From steam drum to downcomer
11.	$(\text{Local losses at steam exit})_P = (\text{Local losses at steam exit})_M$	From interface to steam drum exit piping
12.	$\left(\frac{\text{Steam Drum length}}{\text{Steam drum diameter}}\right)_P = \left(\frac{\text{Steam Drum length}}{\text{Steam drum diameter}}\right)_M$	Ratio of steam drum length and diameter
13.	$\left(\frac{\text{Baffle Height}}{\text{Steam drum diameter}}\right)_P = \left(\frac{\text{Baffle Height}}{\text{Steam drum diameter}}\right)_M$	Ratio of baffle height and Steam drum diameter



**Table 2: Comparison of different dimensions of prototype and Model SD**

Description	Prototype		Model
	Latest design (Fig. 2b)	Earlier version (Fig. 2a)	
Number of tail pipes for 1/8 <sup>th</sup> section of SD	14	14	15
Tail pipe internal diameter (mm)	110.0	122.24	62.7
Steam drum inside diameter (mm)	4000.0	3750.0	1916.2
Steam drum length for 28 channels (mm)	2250.0	2250.0	1154.0
Baffle spacing (mm)	1000.0	1000.0	423.0
Baffle height (mm)	0.5340	450.0	194.9
Interface level (mm)	2200.0	2070.0	1013.5
Height of steam space (mm)	1800.0	1650.0	902.7
Number of downcomers for 1/8 <sup>th</sup> section of SD	1	1	1
Downcomer internal diameter (mm)	273.1	288.89	134.5
Steam drum volume per unit length (m <sup>3</sup> /m)	12.566	11.044	2.883

**Table 3: Comparison of scaling parameters for prototype and model.**

Sr. No.	Parameters for scaling	Prototype-1 (with 3.75 m diameter)	Model	Prototype-2 (with 4 m dia)	Deviation of model with prototype - 2 (%)
1.	$(J_{G-TP})$	2.1020	2.1020	2.607	-19.37
2.	$(J_{L-TP})$	0.4840	0.4840	0.5454	-11.25
3.	$\left(\frac{\text{Tail pipe pitch}}{\text{Tail pipe dia}}\right)$	3.2376	3.2376	3.5454	-8.68
4.	$(\text{Entry losses in steam drum})$	0.8203	0.8203	0.8584	- 4.43
5.	$(J_{G-R})$	0.1980	0.1980	0.1922	+ 3.06

6.	$(J_{L-R})$	0.0456	0.0456	0.0400	+ 13.82
7.	$(J_{G-IF})$	0.0823	0.0823	0.0896	- 8.12
8.	$(J_{L-BI})$	0.0456	0.0456	0.0446	+ 2.13
9.	$(J_{L-BS})$	0.0858	0.0858	0.0918	- 6.62
10.	$(Local\ losses\ at\ downcomer)$	0.4890	0.4890	0.4886	- 0.07
11.	$(Local\ losses\ at\ steam\ exit)$	0.4994	0.4994	0.4996	- 0.03
12.	$\left(\frac{Steam\ Drum\ length}{Steam\ drum\ dia}\right)$	0.5979	0.5979	0.4875	+ 22.60
13.	$\left(\frac{Baffle\ Height}{Steam\ drum\ dia}\right)$	0.1196	0.1196	0.1335	- 10.39

**Table 4: Sizing of different components of AWL**

Sr. No.	Component	No.s.	Average length (m)	Size/Diameter (m)	Material
1	Vertical feeder	15	3.6	0.0627	SS 304 L
2	Horizontal feeder	15	5.0	0.0627	SS 304 L
3	Tail pipe (1-Ø)	15	0.5	0.0627	SS 304 L
4	Tail pipe (2-Ø)	15	4.5	0.0627	Acrylic
5	Steam drum	1	1.154	1.916	Acrylic
6	Loop downcomer pipe	1	2.0	0.1345	Acrylic
7	Horizontal downcomer	1	5.0	0.1345	SS 304 L
8	Vertical downcomer	1	2.0	0.1345	Acrylic
9	Storage tank	1	1.5	1.2m×1.2m	SS 304 L

## 8.0 Experimental Programs

The experiments are planned in the following different phases

- Experiments for Carryover and Carryunder along with swell level measurement in steam drum.
- Experiments for flow pattern studies in vertical tail pipes
- Experiments with specified variation of air injection at different tail pipes.

## 9.0 Instrumentation and parameters to be measured

The different parameters to be measured are as follows

- **Air-Water Drum:** Pressure, swell level, pool void fraction and exit entrainment
- **Tail pipes:** Flow rate and pressure drop
- **Downcomer:** Flow rate and pressure drop
- **Entrainment:** Bubble and droplet size

The measurements carried out are as follows:

- **Swell** in the air-water drum is measured by change in measured levels with and without air injection.
- **Flow** measurement in the single-phase horizontal pipe is carried out by calibrated pipe taps (pipe flow meter).
- **Pressure drop and level measurement** is done with differential pressure transducers or transmitters.
- **Pressure measurement** in the steam drum is carried out using pressure transducer.
- **Entrainment (carryover & Carryunder)** is obtained by measuring separated water and High Speed Videography.

## 10.0 Pre-test analysis

### 10.1 Steady state flow analysis

Steady state analysis has been carried out for determining the superficial velocities of phases across various sections of the loop. For this purpose loop is simulated as a simple closed loop. The different components of the loop have been modeled as shown in Fig. 8. All the tail pipes have been lumped in to a single pipe. The following steady state equation has been solved iteratively for finding out the flow through loop.

$$\Delta P_{1-\phi} + \Delta P_{2-\phi} = -g \oint \rho dz \quad (1)$$

Where,

$$\Delta P_{1-\phi} = \sum_{i=1}^3 \left( \frac{fL}{D_i A_i^2} + \frac{K_i}{A_i^2} \right)_i \frac{W_w^2}{2\rho_w} + \sum_{i=7}^{11} \left( \frac{fL}{D_i A_i^2} + \frac{K_i}{A_i^2} \right)_i \frac{W_w^2}{2\rho_w} \quad (2)$$

$$\Delta P_{2-\phi} = \sum_{i=4}^6 \left( \frac{fL}{D_i A_i^2} + \frac{K_i}{A_i^2} \right)_i \frac{W_T^2}{2\rho_{av}} \quad (3)$$

$f$  is calculated based on the Reynolds number estimated assuming the total flow to be water,  $K$  is the local loss coefficient based on the area changed and the  $\rho_{av}$  is estimated as follows

$$\rho_{av} = (1 - \alpha)\rho_w + \alpha\rho_g \quad (4)$$

Initially, the required flow rate of air and water for the model was given as input. The pressure drops in single-phase and two-phase regions were calculated. The lengths of the different pipes were found out so that the equation (1) was satisfied. For the subsequent analysis, the lengths of different pipes were fixed as obtained in the first part. The length and sizes of the different components of the loop are tabulated in Table-4. For particular air flow rate the water flow was found out from equations (1) to (3) iteratively. The steady state water flow rate is first assumed

and pressure drops in various sections of the loop are calculated. For calculation of two phase density and two phase pressure drop, void fraction correlation is required. The void fraction in tail pipe is determined by Chexal-Lellouche correlation<sup>3</sup>. The void fraction in the steam drum pool is calculated from Kataoka & Ishii model<sup>4</sup>.

## 10.2 Carryover analysis

Ishii and Grolmes<sup>5</sup> have proposed the entrainment at the surface of pool as a function of physical properties.

$$E_{LG} = f\left(\frac{\Delta\rho}{\rho_G}\right) \quad (5)$$

Where,  $E_{LG}$  is the entrainment fraction defined as,

$$E_{LG} = \frac{\rho_L V_{LG}}{\rho_G V_G} \quad (6)$$

and, the entrainment rate  $\varepsilon_{LG}$  is given by,

$$\varepsilon_{LG} = E_{LG} \rho_G V_G \quad (7)$$

$$\Delta\rho = \rho_L - \rho_G \quad (8)$$

$V_{LG}$  the entrained droplet flux.

Ishii and Grolmes<sup>5</sup> proposed the maximum droplet size based on the mechanism of droplet formation by bursting of bubbles, based on the pool entrainment theory as,

$$d_{\max}^* = C v_G^{*-n} \quad (9)$$

Where,  $d_{\max}^*$  and  $v_G^*$  are the dimensionless maximum droplet diameter and superficial gas velocity given by,

$$d_{\max}^* = \frac{d}{\sqrt{(\sigma/(g\Delta\rho))}} \quad (10)$$

$$v_G^* = \frac{v_G}{(\sigma g \Delta \rho / \rho_G^2)^{1/4}} \quad (11)$$

$C$  and  $n$  are constants obtained experimentally by Ishii for wide range of pressures.

Mugele and Evans<sup>6</sup> proposed that Upper Limit Log Normal (ULLN) distribution function is most convenient to use. The ULLN is basically a normal distribution function with transformed variable. The normal density function for a variable is given by

$$f(\eta) = \frac{\delta}{\pi} \exp(-\delta^2 \eta^2) \quad (12)$$

Where  $\eta$  is transformed variable

$$f(\eta) = f(d) \left| \frac{\partial d}{\partial \eta} \right| \quad (13)$$

$$f(d) = \frac{\delta d_{\max}}{\sqrt{\pi} d (d_{\max} - d)} \exp \left[ -\delta^2 \left\{ \ln \left( \frac{ad}{d_{\max} - d} \right) \right\}^2 \right] \quad (14)$$

Where  $a$  and  $\delta$  are the size and distribution parameters respectively.

Droplet trajectory is analyzed for all the sizes of droplet, under the assumption that only drag and buoyancy are acting together.

$$\frac{dv_d}{dt} = -\frac{\Delta\rho}{\rho_L} g - \frac{3}{4} C_d \frac{1}{d} \frac{\rho_G}{\rho_L} (v_d - v_G) |v_d - v_G| \quad (15)$$

Where  $C_d$  is given by,

$$C_d = \frac{24}{\text{Re}_d} \text{ for } \text{Re}_d \leq 1 \quad (16)$$

$$C_d = \frac{18.5}{\text{Re}_d^{0.5}} \text{ for } 1 < \text{Re}_d \leq 500 \quad (17)$$

$$C_d = 0.44 \text{ for } 500 < \text{Re}_d < 200000 \quad (18)$$

If  $d_{cr}$  is the diameter of the largest droplet reaching at given height of drier ( $h = h_{sd}$ ) then entrainment at drier can be written as:

$$\mathcal{E}_{LG(h=h_{sd})} = K \int_0^{d_{cr}} \frac{\pi}{6} \rho_L d^3 f(d) dd \quad (19)$$

Where  $K$  is obtained from

$$K = \frac{\mathcal{E}_{LG(h=0)}}{\int_0^{d_{max}} \frac{\pi}{6} \rho_L d^3 f(d) dd} \quad (20)$$

### 10.3 Carryunder analysis

Computer code GSEP-CU for carryunder<sup>2</sup> was used for the carryunder analysis. Carryunder analysis was carried out for both the model and prototype with air-water. This code uses Petrick's model<sup>7</sup> based on assumption of semi-circular trajectory of liquid particles. Poisson's distribution is employed for bubble size distribution. Bubble trajectory is analyzed to obtain the maximum bubble size carried to downcomer.

For the bubble trajectory analysis the liquid flowing from riser to downcomer can be assumed to describe circular streamlines, for large interface height ratio  $H/D_{DC} > 1$  as observed by Petrick<sup>7</sup>.

First and foremost condition for bubble to get entrained in downcomer is that, its absolute velocity should be directed downward, which requires its terminal velocity to be lower than liquid velocity in downcomer. Terminal velocity of a bubble is given as:

$$V_0 = \sqrt{\frac{4(\rho_L - \rho_G)gd}{3\rho_L C_d}} \quad (20)$$

Another entrainment condition arises from the fact that the trajectory must fall in the downcomer. This condition provides, the pseudo area in the riser causing the carryunder. Carryunder prediction comprises of evaluating the volume fraction of the bubbles that could be entrained on account of first entrainment condition and evaluation of pseudo area contributing to carryunder based on second entrainment condition. At low interface height, some of the bubble trajectories arising from pseudo area of riser may intercept the free surface and cause the bubble to escape and reduce carryunder. On the other hand at low interface heights higher gas velocity due to lower cross-sectional flow area may have the effect of increasing the carryunder. This requires accounting two competing effects of height on carryunder.



## 11.0 Results and discussions

The predicted variation of steady state air and water flow rates with void fraction is shown in Fig. 9 and 10 respectively. From these Fig.s it is seen that as expected the initial air flow rate required increases slowly with void fraction and increases sharply for large void fraction. The induced water flow rate increases steeply at low values of void fraction and increases marginally at higher void fraction.

The variation of void fraction in tail pipes, steam drum riser and steam drum pool are plotted against total flow rate in Fig. 11. From these Fig.s it can be seen that for the lower values total flow rates void fraction increase rate is lower for all the locations mentioned above. Increase in void fraction is higher at higher flow rates. For every flow rate the void fraction predicted in the tail pipe is the largest while in the pool it is lowest.

The superficial velocities in the tail pipe, steam drum riser and steam drum were also estimated for model and prototype geometries. The variation of void fraction with air superficial velocity in tail pipe is shown in Fig. 12. The variation of void fraction with air superficial velocity is nearly same for the model and prototype.

The variation of void fraction with air superficial velocity in the steam drum riser is shown in Fig. 13. There is substantial difference in variation of void fraction in model and prototype steam drum riser which can be attributed to the variation in curvature of steam drum inside surface. The variation in flow area as the flow moves towards the steam drum pool portion is different for model and prototype steam drum.

The variation of void fraction with air superficial velocity across the steam water interface is shown in Fig. 14. The void fraction variation is identical in model and prototype steam drum.

Fig. 15 shows the variation of critical droplet diameter and maximum droplet diameter with air velocity in model and prototype steam drum. The maximum droplet diameter decreases with air velocity while the critical droplet diameter increases with air velocity. Two different entrainment

zones are identified as Zone-I and Zone-II. In the Zone-I at lower air velocities the critical droplet diameter governs and effective gravity separation is obtained. As the air velocity increases in the Zone-II, the maximum droplet diameter available decreases lower than the critical droplet diameter and all the droplets are thus entrained in the gas flow. In Zone-II the gravity separation is not effective and entrainment is governed by the maximum droplet diameter. From Fig. 15 it can be seen that entrainment maps are identical for model and prototype steam drum.

In Fig. 16 the variation of carryover with the air velocity is plotted for both the model and prototype steam drum. From the Fig. it can be seen that the carryover is negligible at the low air velocities and increases sharply at higher air velocities. After certain velocities the carryover is equal to the amount of entrainment at the interface. From the Fig. we can conclude that the nature of carryover is same for both the model and prototype steam drum. Only difference is the velocity at which there is sharp rise in the carryover.

Fig. 17 shows the variation of carryunder with the downcomer velocity for model and prototype steam drum. The effect of quality is also plotted on the same curve. From this Fig. it can be seen that carryunder initially increases sharply at lower downcomer velocities because with increasing downcomer velocity the maximum size of bubble that can be entrained increases sharply. On the other hand, beyond certain velocity, the maximum size of bubble carried is equal to largest bubble in the riser. At higher velocities the carryunder remains constant/steady. It can be also seen that at higher flow qualities the carryunder is high. It is because more bubbles form at the higher quality

## **12.0 Concluding Remarks**

An Air-Water Loop has been designed, fabricated, installed and commissioned at Engineering Hall-7, BARC, with aim to carry out experiments for investigation of carryover and carryunder phenomena in gravity separation of two-phase flow relevant to AHWR steam drum. The scaling has been carried out to preserve the important criterion such as superficial velocities of phases at various cross-sections of the model and prototype, local momentum losses, geometric constraints

like pitch of tail pipes, baffle height to steam drum diameter ratio and steam drum diameter to length ratio. The scaling philosophy, results of steady state analysis, carryunder and carryover analysis are presented for model and prototype. Tail pipe void fraction can be simulated with appropriate air flow rates. Experiments on steady state two-phase natural circulation, measurement of carryover and pool void fraction are in progress.

## **Nomenclature**

$A$	:	Cross-section flow area ( $m^2$ )
$A_R$	:	Area ration
$B$	:	Baffle
$B_s$	:	Baffle spacing (m)
$d$	:	Pipe diameter (m)
$D$	:	Diameter (m)
$G$	:	Mass flux ( $kg/m^2s$ )
$H$	:	Height (m)
$J$	:	Volumetric flux (m/s)
$K_I$	:	Inlet loss coefficient
$K_E$	:	Exit loss coefficient
$L$	:	Length (m)
$m$	:	Mass flow rate (kg/s)
$P$	:	Pitch (m)
$Q$	:	Volumetric flow rate ( $m^3/s$ )
$x$	:	Flow quality

## **Greek Symbols**

$\rho$	:	Density ( $kg/m^3$ )
--------	---	----------------------

### ***Subscripts***

<i>a</i>	:	Air
<i>BI</i>	:	Baffle interface
<i>BS</i>	:	Baffle space
<i>g</i>	:	Gas
<i>H</i>	:	Height
<i>IF</i>	:	Interface
<i>L</i>	:	Liquid
<i>M</i>	;	Model
<i>P</i>	;	Prototype
<i>R</i>	:	Riser
<i>s</i>	:	Steam
<i>SD</i>	:	Steam drum
<i>T</i>	:	Total
<i>TP</i>	:	Two phase
<i>TDC</i>	:	Total downcomer
<i>w</i>	:	Water

### **References**

1. Nayak, A. K., Jain, V., Vijayan, P. K., Saha, D. and Sinha, R. K., “Study of carryover behavior in the steam drum of the advanced heavy water reactor”, Proceedings of the Sixteenth National Convention of Mechanical Engineers and National Seminar on Future trends in Mechanical Engineering, Research and Development, Deptt. Of Mech. And Ind. Engg., UOR, Roorkee, Sept. 29-30, 2000.
2. Jain, V., Nayak, A. K., Vijayan, P. K., Saha, D. and Sinha, R. K., “Modelling of the carryunder phenomena in the steam drum of the advanced heavy water reactor”, Proceedings of Fifth ISHMT-ASME Heat and Mass Transfer Conference and Sixteenth National Heat and Mass Transfer Conference, Science City, Kolkata, January 3-5, 2002.

3. Chexal, B., Maulbetsch, J., Santucci, J., Harrison, J., Jensen, P., Peterson, C., Lellouche, G. and Horowitz, J., 1996, "Understanding void fraction in steady and dynamic environments", TR-106326/RP-8034-14, Electric Power Research Institute, 3412 Hillview Avenue, California.
4. Kataoka, I. and Ishii, M., 1987, "Drift flux model for large diameter pipe and new correlation for pool void fraction", *Heat and Mass Transfer*, 30 (9), 1927-1939.
5. Ishii, M. and Grolmes, M.A. (1975), "Inception criteria for droplet entrainment in two-phase concurrent film flow", *AIChE Journal*, Vol. 21, no. 2, pp. 308-318.
6. Mugele, R. A. and Evans, H. D., (1951), "Droplet size distribution in sprays", *Industrial and Engineering Chemistry*, Vol. 43, No. 6, pp. 1317-1324.
7. Petrick Michael, "A study of vapor carryunder and associated problems", ANL-6581, July 1962.

## APPENDIX-A: SIZING OF VARIOUS COMPONENTS OF AWL

### Prototype to model scaling ratio

Reactor operating conditions are as follows:

Total mass flow rate through core (452 channels) = 2306.0 kg/s

Total Mass flow rate per steam drum (113 channels) = 576.5 kg/s

Total Mass flow rate for 28 channels =  $m_T = 142.85$  kg/s.

Steam flow rate for 452 channels = 405.0 kg/s.

Steam flow rate for 28 channels =  $m_s = 405.0 \times 28 \div 452 = 25.088$  kg/s.

Volumetric steam flow rate for 28 channels of prototype =  $(Q_s)_p = 25.088 \div 36.32$   
=  $0.69075$  m<sup>3</sup>/s = 41445 lpm.

Water flow rate for 28 channels of prototype =  $m_w = m_T - m_s = 142.85 - 25.088 = 117.76$  kg/s

Volumetric water flow rate for 28 channels of prototype =  $(Q_L)_p = 0.1591$  m<sup>3</sup>/s.

Flow quality =  $x = \frac{m_s}{m_T} = 25.088 \div 142.85 = 0.1756$

Air flow available in Hall-7 = 600 SCFM at 1 atm. =  $600 \times 28.31 = 16986.0$  lpm at 1 atm.

Maximum flow scaling that can be obtained as =  $16986.0 \div 41445.0 = 1/2.453$

Scaling assumed for sizing of components = 1/4

Therefore, the required air at atmospheric pressure =  $41445.0/4 = 10361.25$  lpm

To maintain the superficial velocities of gaseous and liquid phases at various locations in prototype and model as equal, it is evident that the flow areas also shall be scaled. Fig. A-1 shows the simplified cross-sectional view of prototype steam drum.

From Fig. A-1,

$$OC = \sqrt{OA^2 - AC^2} = \sqrt{1.875^2 - 0.5^2} = 1.807 \text{ m}$$

$$BC = OB - OC = 1.875 - 1.807 = 0.068 \text{ m}$$

$$BD = BC + CD = 0.068 + 0.450 = 0.518 \text{ m}$$

$$OD = OB - BD = 1.875 - 0.518 = 1.357 \text{ m}$$

$$EF = \left( \sqrt{OF^2 - OD^2} \right) - DE = \left( \sqrt{1.875^2 - 1.375^2} \right) - 0.5 = 0.77475 \text{ m}$$

$$GH = \sqrt{OH^2 - OG^2} = \sqrt{1.875^2 - 0.195^2} = 1.8648 \text{ m.}$$

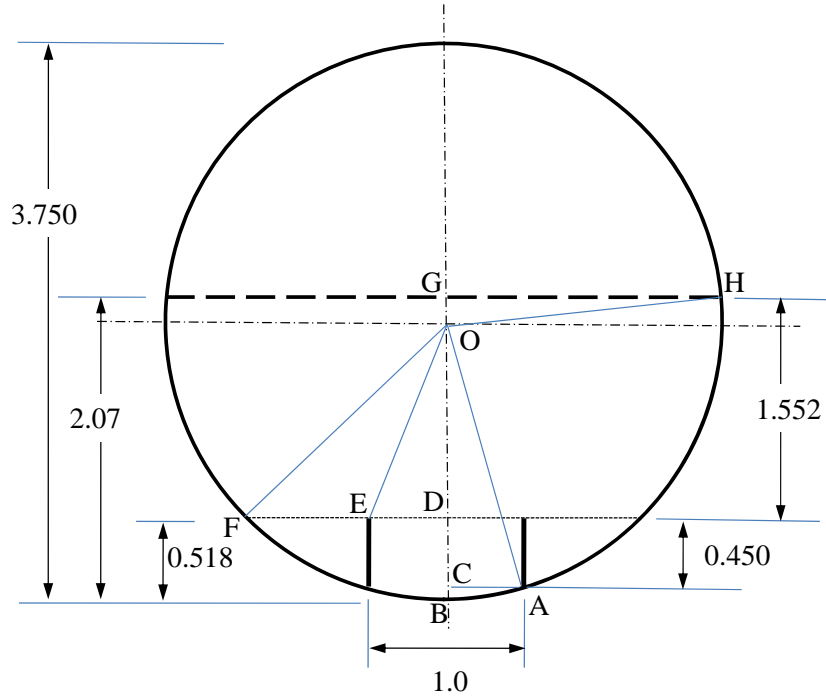


**Fig. A-1: Simplified cross-sectional view of prototype steam drum**

### **Sizing of tail pipe based on superficial velocities of phases**

Tail pipe inside diameter in prototype,  $(d_{TP})_p = 0.12224 \text{ m}$

Flow area of 28 tail pipes,  $(A_{TP})_p = 28.0 \times \frac{\pi}{4} \times 0.12224^2 = 0.3286053 \text{ m}^2$

Mass flux in prototype,  $G = \frac{m_T}{(A_{TP})_p} = 142.85 \div 0.3286053 = 434.72 \text{ kg/m}^2\text{s}$

Superficial velocity of gas in prototype,  $(J_{G-TP})_p = \frac{Gx}{\rho_g} = (434.72 \times 0.1756) \div 36.32 = 2.102 \text{ m/s}$

Superficial velocity of liquid in prototype,  $(J_{L-TP})_p = \frac{G(1-x)}{\rho_l} = (434.72 \times 0.8244) \div 740.19$   
 $= 0.484 \text{ m/s}$

The required flow area in model =  $0.3286053/4 = 0.08215133 \text{ m}^2$

Therefore required ID of a tail pipe in the model =  $\sqrt{\frac{0.0821533}{28} \times \frac{4}{\pi}} = 0.06112 \text{ m}$ .

Nearest available size of pipe is 65 NB Sch. 40 with inside diameter 0.0627 m. Taking tail pipe ID as  $(d_{TP})_M = 0.0627 \text{ m}$ , the flow area for 28 pipes in the model  $(A_{TP})_M = 0.086453582 \text{ m}^2$ .

Keeping the same superficial velocities, i.e.  $(J_{G-TP})_P = 2.102 \text{ m/s}$  and  $(J_{L-TP})_P = 0.484 \text{ m/s}$ .

Volumetric air flow,  $Q_a = (J_{G-TP})_P \times (A_{TP})_M = 2.102 \times 0.086453582$   
 $= 0.18172543 \text{ m}^3/\text{s} = 10903.53 \text{ lpm}$ .

Volumetric water flow,  $Q_w = (J_{L-TP})_P \times (A_{TP})_M = 0.484 \times 0.086453582$   
 $= 0.0418435 \text{ m}^3/\text{s} = 2510.61 \text{ lpm}$ .

#### **Tail pipe pitch and tail pipe diameter in the model**

For  $\left(\frac{\text{Pitch}}{\text{Tail pipe dia}}\right)_P = \left(\frac{\text{Pitch}}{\text{Tail pipe dia}}\right)_M \quad \frac{(P)_P}{(d_{TP})_P} = \frac{(P)_M}{(d_{TP})_M}$

$(P)_M = \frac{(P)_P}{(d_{TP})_P} (d_{TP})_M \Rightarrow (P)_M = \frac{0.0627}{0.12224} \times 0.450$

$(P)_M = 0.2308 \text{ m}$ .

With a pitch of 0.2308 m the length of steam drum,  $(P)_M = 5 \times 0.2308 = 1.154 \text{ m}$

#### **Sizing of steam drum riser portion based on entry losses (Tail pipe to steam drum) and superficial velocities of phases.**

For steam drum riser in prototype at baffle's top,  $(2 \times EF)_P = 2 \times 0.77475 = 1.5495 \text{ m}$ .

Flow area in riser portion (at the top of baffle plates) of prototype,  $(A_R)_P = 1.5495 \times 2.25 = 3.486375 \text{ m}^2$ .

To keep entry losses in the drum same in model and prototype i.e.

$(\text{Entry losses into the drum})_P = (\text{Entry losses into the drum})_M$



$$(K_I)_P = (K_I)_M \Rightarrow \left[1 - \frac{(A_{TP})_P}{(A_R)_P}\right]^2 = \left[1 - \frac{(A_{TP})_M}{(A_R)_M}\right]^2 \Rightarrow \frac{(A_{TP})_P}{(A_R)_P} = \frac{(A_{TP})_M}{(A_R)_M} \Rightarrow (A_R)_M = \frac{(A_{TP})_M}{(A_{TP})_P} (A_R)_P$$

$$(A_R)_M = \frac{0.08645352}{0.3286053} \times 3.486 = 0.9171397 \text{ m}^2$$

$$\text{Superficial velocity of gas in prototype, } (J_{G-R})_P = \frac{Q_s}{(A_R)_P} = \frac{0.6907}{3.486375} = 0.1981 \text{ m/s}$$

$$\text{Superficial velocity of gas in model, } (J_{G-R})_M = \frac{Q_a}{(A_R)_M} = \frac{0.18172543}{0.9171397} = 0.1981 \text{ m/s}$$

$$\text{Superficial velocity of liquid in prototype, } (J_{L-R})_P = \frac{Q_L}{(A_R)_P} = \frac{0.1591}{3.486375} = 0.0456 \text{ m/s}$$

$$\text{Superficial velocity of liquid in the model } (J_{L-R})_M = \frac{Q_w}{(A_R)_M} = \frac{0.0418435}{0.9171397} = 0.0456 \text{ m/s}$$

Thus the superficial velocity of liquid and gas in riser region at top of baffle plate would be conserved if  $(A_R)_M = 0.917238903 \text{ m}^2$

$$\text{Now, } (2 \times EF)_M = \frac{(A_R)_M}{(L_{SD})_M} = \frac{0.9171397}{1.154} = 0.795 \text{ m}$$

### **Sizing of interface area (at gravity separation of phases) based on superficial velocities of phases.**

$$\text{For steam drum at interface in prototype, } (2 \times GH)_P = 2 \times 1.8648 = 3.7296 \text{ m}$$

$$\text{Interface area in SD of prototype, } (A_{IF})_P = 3.7296 \times 2.25 = 8.3916 \text{ m}^2$$

Superficial velocity of gas at interface of steam and water separation,

$$(J_{G-IF})_P = \frac{(Q_s)_P}{(A_{IF})_P} = \frac{0.6907}{8.3916} = 0.0823 \text{ m/s}$$

$$\text{Volumetric air flow rate in the model, } Q_a = 10903.53 \text{ lpm} = 0.18172543 \text{ m}^3/\text{s}$$

For maintaining superficial gas velocity at interface equal in model and prototype,

$$(J_{G-IF})_P = (J_{G-IF})_M \Rightarrow (A_{IF})_M = \frac{Q_a}{(J_{G-IF})_P} = \frac{0.18172543}{0.0823} = 2.2080 \text{ m}^2$$

For steam water interface in model  $(2 \times GH)_M = \frac{(A_{IF})_M}{(L_{SD})_M} = \frac{2.2080854}{1.154} = 1.913 \text{ m}$

**Sizing of phase separation interface height and cross flow area based on superficial velocities of phases.**

Cross flow area in steam drum above baffle plates of prototype (i.e. between the riser top to the steam water separation interface),  $(A_{BI})_P = 2.25 \times (2.07 - 0.518) = 3.492 \text{ m}^2$

Superficial velocity of liquid,  $(J_{L-BI})_P = \frac{(Q_l)_P}{(A_{BI})_P} = \frac{0.1591}{3.492} = 0.0456 \text{ m/s}$

For scaling of cross flow area,

$$(J_{L-BI})_P = (J_{L-BI})_M \Rightarrow (A_{BI})_M = \frac{(Q_l)_M}{(J_{L-BI})_P} = \frac{0.0418435}{0.0456} = 0.917620614 \text{ m}^2$$

Interface height from baffle top in model,  $(H_{BI})_M = \frac{(A_{BI})_M}{(L_{SD})_M} = \frac{0.917620614}{1.154} = 0.796 \text{ m}$

**Sizing of steam drum downcomer region based on superficial velocity of liquid phase.**

Baffle spacing in prototype,  $(B_S)_P = 1.0 \text{ m}$

Baffle length,  $(L_S)_P = 2.25 \text{ m}$

Flow area between baffle spacing,  $(A_{BS})_P = 2.25 \times 1.0 = 2.25 \text{ m}^2$

Total downcomer flow rate,  $(Q_{TDC})_P = \frac{142.85}{740.19} = 0.192990988 \text{ m}^3/\text{s}$

Superficial velocity of liquid,  $(J_{L-BS})_P = \frac{(Q_{DC})_P}{(A_{BS})_P} = \frac{0.192990988}{2.25} = 0.0858 \text{ m/s}$

For maintaining liquid superficial velocity in downcomer region same in model and prototype,

$$(J_{L-BS})_P = (J_{L-BS})_M \Rightarrow (A_{BS})_M = \frac{(Q_{TDC})_M}{(J_{L-BS})_P} = \frac{0.0418435}{0.0858} = 0.48768648 \text{ m}^2$$

Baffle spacing in model,  $(B_S)_M = \frac{(A_{BS})_M}{(L_{SD})_M} = \frac{0.48768648}{1.154} = 0.423 \text{ m}$

### Sizing of downcomer pipe based on exit losses.

Downcomer pipe ID in prototype,  $(d_{DC})_P = 0.28889$  m

Flow area of down comer pipe in prototype,  $(A_{DC})_P = \frac{\pi}{4} \times 0.28889^2 = 0.065547313$  m<sup>2</sup>

For scaling

$$(Exit\ losses\ from\ the\ drum\ to\ downcomer)_P = (Exit\ losses\ from\ the\ drum\ to\ downcomer)_M$$

$$(K_E)_P = (K_E)_M \Rightarrow 0.5 \left[ 1 - \frac{(A_{DC})_P}{(A_{BS})_P} \right]^{0.75} = 0.5 \left[ 1 - \frac{(A_{DC})_M}{(A_{BS})_M} \right]^{0.75} \Rightarrow \frac{(A_{DC})_P}{(A_{BS})_P} = \frac{(A_{DC})_M}{(A_{BS})_M}$$

$$(A_{DC})_M = \frac{(A_{DC})_P}{(A_{BS})_P} (A_{BS})_M = \frac{0.065547313}{2.25} \times 0.4876848 = 0.01420735 \text{ m}^2$$

Therefore required ID of the down comer pipe in the model;

$$(d_{DC})_M = \sqrt{0.01420735 \times \frac{4}{\pi}} = 0.134496692 \text{ m}$$

Nearest available pipe is 125 NB Sch 10 with ID=0.1345 m.

### Sizing of exit pipe based on exit losses.

Steam exit pipe ID in prototype,  $(d_{SE})_P = 0.28889$  m

Flow area of steam exit pipe in prototype,  $(A_{SE})_P = \left( \frac{28}{452} \right) \left( \frac{\pi}{4} \right) (0.28889)^2 = 0.004060453$  m<sup>2</sup>

$$(Exit\ losses\ from\ the\ drum\ to\ steam\ pipe)_P = (Exit\ losses\ from\ the\ drum\ to\ steam\ pipe)_M$$

$$(K_E)_P = (K_E)_M \Rightarrow 0.5 \left[ 1 - \frac{(A_{SE})_P}{(A_{IF})_P} \right]^{0.75} = 0.5 \left[ 1 - \frac{(A_{SE})_M}{(A_{IF})_M} \right]^{0.75} \Rightarrow \frac{(A_{SE})_P}{(A_{IF})_P} = \frac{(A_{SE})_M}{(A_{IF})_M}$$

$$(A_{SE})_M = \frac{(A_{SE})_P}{(A_{IF})_P} (A_{IF})_M = \frac{0.004060453}{8.3916} \times 0.9717238903 = 0.001131731 \text{ m}^2$$

Therefore, the required ID of a air exit pipe in the model;

$$(d_{SE})_M = \sqrt{0.001131731 \times \frac{4}{\pi}} = 0.03796 \text{ m}$$

Nearest available size of pipe is 40 NB Sch 40 with ID = 0.0409 m.

**Sizing of steam drum diameter based on ratio of steam drum length to drum diameter.**

$$\left( \frac{\text{Steam Drum length}}{\text{Steam drum dia}} \right)_P = \left( \frac{\text{Steam Drum length}}{\text{Steam drum dia}} \right)_M$$

$$\frac{(L_{SD})_P}{(D_{SD})_P} = \frac{(L_{SD})_M}{(D_{SD})_M} \Rightarrow (D_{SD})_M = \frac{(L_{SD})_M}{(L_{SD})_P} (D_{SD})_P = \frac{1.154}{2.25} \times 3.75$$

$$(D_{SD})_M = 1.924 \text{ m.}$$

**Sizing of baffle height based on ratio of baffle plate height to drum diameter.**

$$\left( \frac{\text{Baffle Height}}{\text{Steam drum dia}} \right)_P = \left( \frac{\text{Baffle Height}}{\text{Steam drum dia}} \right)_M$$

Therefore m

$$\frac{(B_H)_P}{(D_{SD})_P} = \frac{(B_H)_M}{(D_{SD})_M} \Rightarrow (B_H)_M = \frac{(B_H)_P}{(D_{SD})_P} (D_{SD})_M = \frac{0.45}{3.75} \times 1.924$$

$$(B_H)_M = 0.23088 \text{ m.}$$

The cross-sectional area of AWL steam drum is shown in Fig. A-2 as below

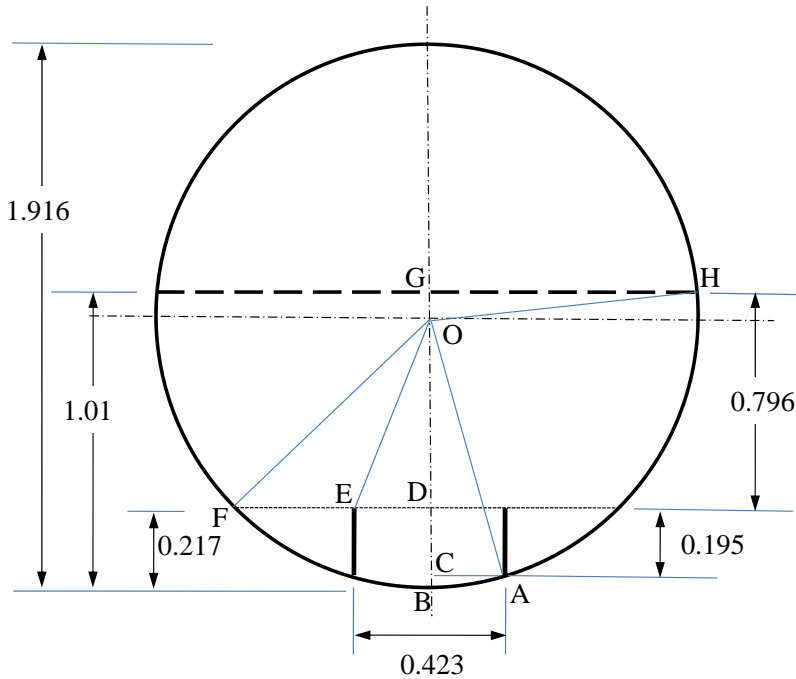


**Fig. A-2: Cross-sectional area of model steam drum**

Though the steam drum diameter and baffle plate height calculated as above are 1.924 m and 0.230 m respectively, but to keep the consistency in the other parameters and overall dimensions of the steam drum and associated piping, these were taken as 1.916 m and 0.195 m respectively.

## APPENDIX-B: Applicability of AWL scaling to the latest design of AHWR steam drum

According to the specifications of the latest design of AHWR:

Total core flow rate (452 channels) = 2141 kg/s.

Total mass flow rate per steam drum (113 channels) = 535.25 kg/s.

Total mass flow rate for 28 channels =  $m_T = 132.63$  kg/s.

Steam flow rate for 452 channels = 408.0 kg/s.

Steam flow rate for 28 channels =  $m_s = 408.0 \times 28 \div 452 = 25.274$  kg/s.

Volumetric steam flow rate for 28 channels of prototype =  $(Q_s)_p = 25.274 \div 36.32$   
=  $0.69587 \text{ m}^3/\text{s} = 41752.20 \text{ lpm}$ .

Average core exit quality = 19.1%.

Water flow rate for 28 channels of prototype =  $m_w = m_T - m_s = 132.63 - 25.274 = 107.356$  kg/s

Volumetric water flow rate for 28 channels of prototype =  $(Q_L)_p = 107.356 \div 740.16 = 0.14504$   
 $\text{m}^3/\text{s}$ .

Steam drum diameter of prototype =  $(D_{SD})_p = 4.0$  m

Prototype steam drum length =  $(L_{SD})_p = 11.0$  m.

Tail pipe ID in prototype =  $(D_{TP})_p = 0.110$  m.

A simplified cross-section of the steam drum is as shown in Fig. B-1.

From Fig. B-1,

$$OC = \sqrt{OA^2 - AC^2} = \sqrt{2.0^2 - 0.5^2} = 1.936 \text{ m}$$

$$BC = OB - OC = 2.0 - 1.936 = 0.064 \text{ m}$$

$$BD = BC + CD = 0.064 + 0.534 = 0.6 \text{ m}$$

$$OD = OB - BD = 2.0 - 0.6 = 1.4 \text{ m}$$

$$EF = \left( \sqrt{OF^2 - OD^2} \right) - DE = \left( \sqrt{2^2 - 1.4^2} \right) - 0.5 = 0.9283 \text{ m}$$

$$GH = \sqrt{OH^2 - OG^2} = \sqrt{2^2 - 0.2^2} = 1.99 \text{ m}.$$

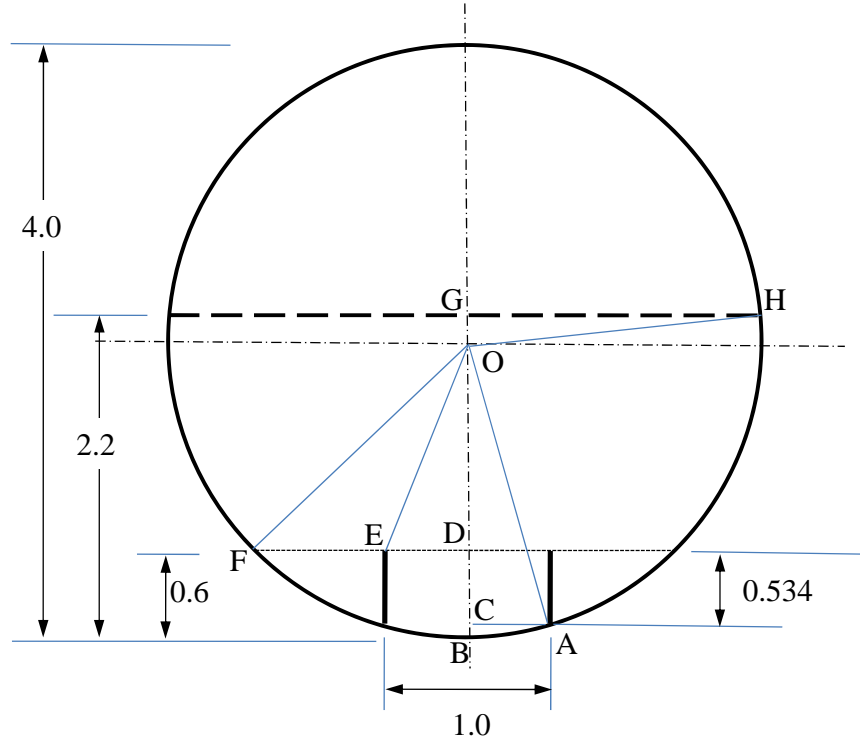


Fig. B-1: Simplified schematic of latest version of prototype steam drum.

### Superficial velocities of phases in tail pipe

Tail pipe inside diameter in prototype,  $(d_{TP})_p = 0.110$  m

Flow area of 28 tail pipes,  $(A_{TP})_p = 28.0 \times \frac{\pi}{4} \times 0.110^2 = 0.26609$  m<sup>2</sup>

Mass flux in prototype,  $G = \frac{m_T}{(A_{TP})_p} = 132.63 \div 0.26609 = 498.435$  kg/m<sup>2</sup>s

Superficial velocity of gas in prototype,  $(J_{G-TP})_p = \frac{Gx}{\rho_g} = (498.435 \times 0.19) \div 36.32 = 2.607$  m/s

Superficial velocity of liquid in prototype,  $(J_{L-TP})_p = \frac{G(1-x)}{\rho_l} = (498.435 \times 0.81) \div 740.19$   
 $= 0.5454$  m/s.

The superficial velocity of gas in model =  $(J_{G-TP})_M = 2.102$  m/s (Refer to Appendix-A)

The superficial velocity of liquid in model =  $(J_{L-TP})_M = 0.484$  m/s (Refer to Appendix-A)

Thus comparing the superficial velocities in model and prototype tail pipes it is found that the simulated gas and liquid superficial velocities deviate from prototype by -19% and -11% respectively.

### **Ratios of Tail pipe pitch and tail pipe diameter in the model and prototype**

$$\left( \frac{\text{Pitch}}{\text{Tail pipe dia}} \right)_P = 0.390 \div 0.110 = 3.5454$$

$$\left( \frac{\text{Pitch}}{\text{Tail pipe dia}} \right)_M = 0.203 \div 0.0627 = 3.2376$$

Thus the above ration in model deviates from prototype by -8.68 %.

### **Entry losses from Tail pipe to steam drum riser portion**

For steam drum riser in prototype at baffle's top,  $(2 \times EF)_P = 2 \times 0.9283 = 1.8566$  m.

Flow area in riser portion (at the top of baffle plates) of prototype,  $(A_R)_P = 1.8566 \times 2.25 = 3.62037$  m<sup>2</sup>.

$$(K_I)_P = \left[ 1 - \frac{(A_{TP})_P}{(A_R)_P} \right]^2 = 0.85840$$

For model,

$$(A_R)_M = 0.917238903 \text{ m}^2 \text{ (refer Appendix-A)}$$

$$(A_{TP})_M = 0.08645 \text{ m}^2$$

$$(K_I)_M = \left[ 1 - \frac{(A_{TP})_M}{(A_R)_M} \right]^2 = 0.8203$$

The local loss coefficient from tail pipe to steam drum riser portion in model deviates from prototype by -4.43% only.

### **Superficial velocities of phases at steam drum riser portion.**

$$\text{Superficial velocity of gas in prototype, } (J_{G-R})_P = \frac{Q_s}{(A_R)_P} = \frac{0.69587}{3.62037} = 0.19220 \text{ m/s}$$



Superficial velocity of gas in model,  $(J_{G-R})_M = \frac{Q_a}{(A_R)_M} = \frac{0.18172543}{0.917238903} = 0.1981 \text{ m/s}$

Superficial velocity of liquid in prototype,  $(J_{L-R})_P = \frac{Q_L}{(A_R)_P} = \frac{0.14504}{3.62037} = 0.04006 \text{ /s}$

Superficial velocity of liquid in the model  $(J_{L-R})_M = \frac{Q_w}{(A_R)_M} = \frac{0.1591}{0.917238903} = 0.0456 \text{ m/s}$

Thus the superficial velocity of gas and liquid at steam drum riser portion for the model deviates from prototype by +3.06% and +13.82 % respectively.

### **Superficial velocity of gas at interface of phase separation.**

For steam drum at interface in prototype,  $(2 \times GH)_P = 2 \times 1.99 = 3.98 \text{ m}$

Interface area in SD of prototype,  $(A_{IF})_P = 3.98 \times 1.950 = 7.761 \text{ m}^2$

Superficial velocity of gas at interface of steam and water separation,

$$(J_{G-IF})_P = \frac{(Q_s)_P}{(A_{IF})_P} = \frac{0.69587}{7.761} = 0.089662 \text{ m/s}$$

Superficial velocity of gas in model at interface =  $(J_{G-IF})_M = 0.0823 \text{ m/s}$  (refer to Appendix-A)

The superficial velocity of gas at interface in model deviates from prototype by -8.21 %.

### **Superficial velocity of liquid at cross flow area above the baffle plate**

Cross flow area in steam drum above baffle plates of prototype (i.e. between the riser top to the steam water separation interface),  $(A_{BI})_P = 1.950 \times (2.2 - 0.534) = 3.2487 \text{ m}^2$

Superficial velocity of liquid,  $(J_{L-BI})_P = \frac{(Q_l)_P}{(A_{BI})_P} = \frac{0.14504}{3.2487} = 0.04464 \text{ m/s}$

Superficial velocity of liquid at cross flow area above baffle plate for the model =  $(J_{L-BI})_M = 0.0456 \text{ m/s}$  (refer to Appendix-A)

Thus the superficial velocity of liquid at cross flow area above baffle plate for the model deviates from the prototype by +2.13 %.

### Superficial velocity of liquid in downcomer region of steam drum

Baffle spacing in prototype,  $(B_s)_p = 1.0$  m

Baffle length,  $(L_s)_p = 1.95$  m

Flow area between baffle spacing,  $(A_{BS})_p = 1.95 \times 1.0 = 1.95$  m<sup>2</sup>

Total downcomer flow rate,  $(Q_{TDC})_p = \frac{132.63}{740.19} = 0.17918$  m<sup>3</sup>/s

Superficial velocity of liquid,  $(J_{L-BS})_p = \frac{(Q_{DC})_p}{(A_{BS})_p} = \frac{0.17918}{1.95} = 0.09187$  m/s

Superficial velocity of liquid in down comer region for model  $= (J_{L-BS})_M = 0.0858$  m/s (refer Appendix-A)

Thus superficial velocity of liquid in down comer region for model deviates from prototype by -6.62 %.

### Local losses in down comer region

Loop downcomer pipe ID in prototype,  $(d_{DC})_p = 0.2731$  m

Flow area of down comer pipe in prototype,  $(A_{DC})_p = \frac{\pi}{4} \times 0.2731^2 = 0.05857783$  m<sup>2</sup>

$$(K_E)_p = 0.5 \left[ 1 - \frac{(A_{DC})_p}{(A_{BS})_p} \right]^{0.75} = 0.5 \left[ 1 - \frac{0.05857783}{1.95} \right]^{0.75} = 0.48869$$

Loop downcomer pipe ID in model,  $(d_{DC})_M = 0.1345$  m

Flow area of down comer pipe in model,  $(A_{DC})_M = \frac{\pi}{4} \times 0.1345^2 = 0.0142080$  m<sup>2</sup>

$$(K_E)_M = 0.5 \left[ 1 - \frac{(A_{DC})_M}{(A_{BS})_M} \right]^{0.75} = 0.5 \left[ 1 - \frac{0.0142080}{0.4876848} \right]^{0.75} = 0.4890$$

Thus the local loss from downcomer region to downcomer pipe in model deviates from prototype by +0.07 %.

### Local loss at exit of steam drum

Steam exit pipe ID in prototype,  $(d_{SE})_p = 0.18258$  m

Flow area of down comer pipe in prototype,

$$(A_{SE})_P = 4.0 * \left( \frac{28}{452} \right) \left( \frac{\pi}{4} \right) (0.18258)^2 = 0.006487477 \text{ m}^2$$

Exit losses from steam drum in prototype

$$(K_E)_P = 0.5 \left[ 1 - \frac{(A_{SE})_P}{(A_{IF})_P} \right]^{0.75} = 0.5 \left[ 1 - \frac{0.006487477}{7.761} \right]^{0.75} = 0.49968$$

Exit losses from stem drum in model

$$(K_E)_M = 0.5 \left[ 1 - \frac{(A_{SE})_M}{(A_{IF})_M} \right]^{0.75} = 0.5 \left[ 1 - \frac{0.00131382}{0.971723} \right]^{0.75} = 0.49949$$

Thus the local losses at steam drum exit for model deviates from prototype by -0.039%.

#### **Ratio of steam drum length to diameter**

$$\left( \frac{\text{Steam Drum length}}{\text{Steam drum dia}} \right)_P = \frac{1.95}{4.0} = 0.4875$$

$$\left( \frac{\text{Steam Drum length}}{\text{Steam drum dia}} \right)_M = \frac{1.154}{1.93} = 0.5979$$

Thus the ratio of steam drum length to steam drum diameter in model deviates from prototype by +22.6 %.

#### **Ratio of baffle height to drum diameter.**

$$\left( \frac{\text{Baffle Height}}{\text{Steam drum dia}} \right)_P = \frac{0.534}{4} = 0.1335$$

$$\left( \frac{\text{Baffle Height}}{\text{Steam drum dia}} \right)_M = \frac{0.23088}{1.93} = 0.119626$$

Thus the ratio of baffle height to drum diameter in model deviates from prototype by -10.39 %.

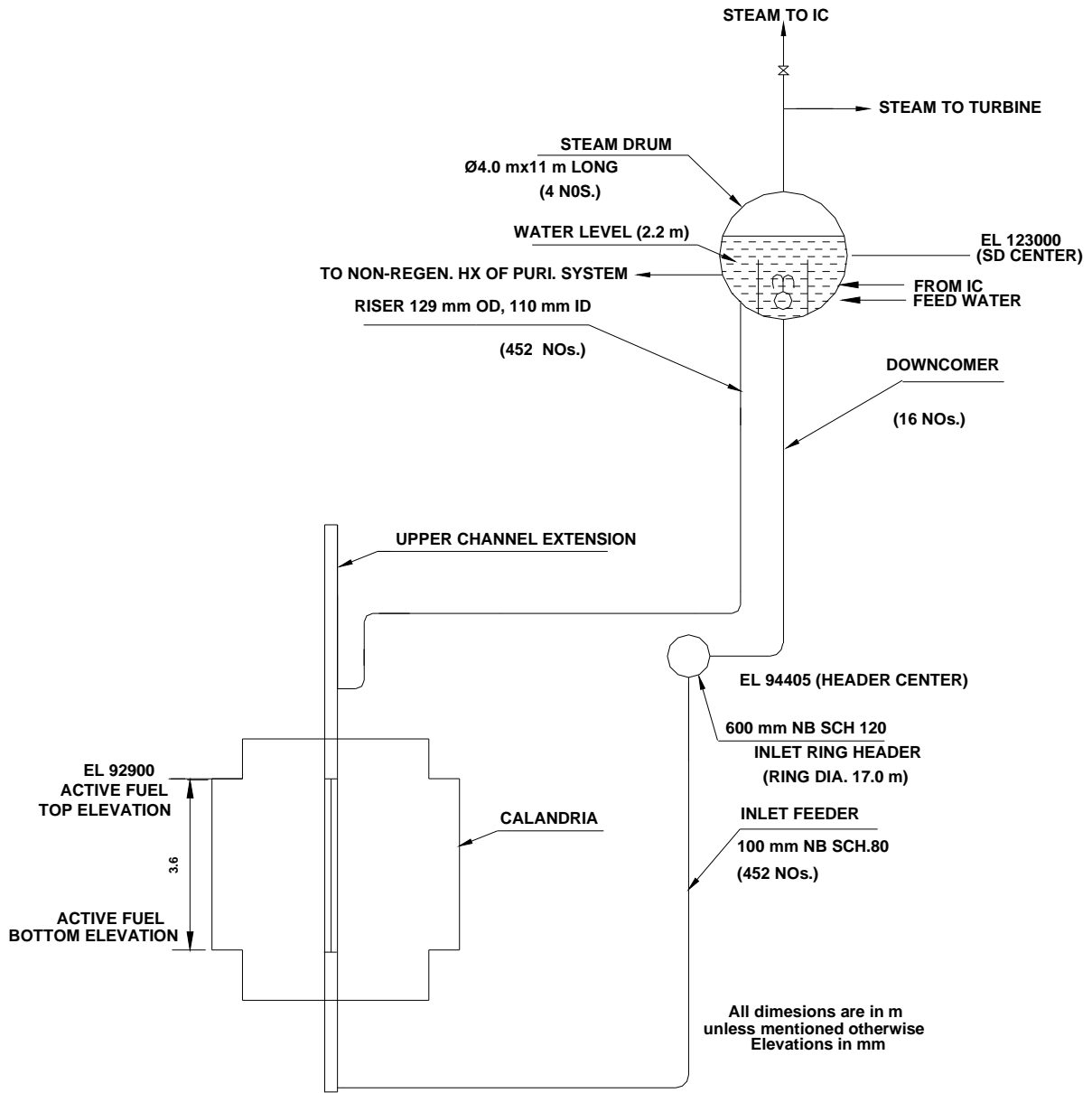


**Fig. 1: Schematic of PHT system of AHWR**

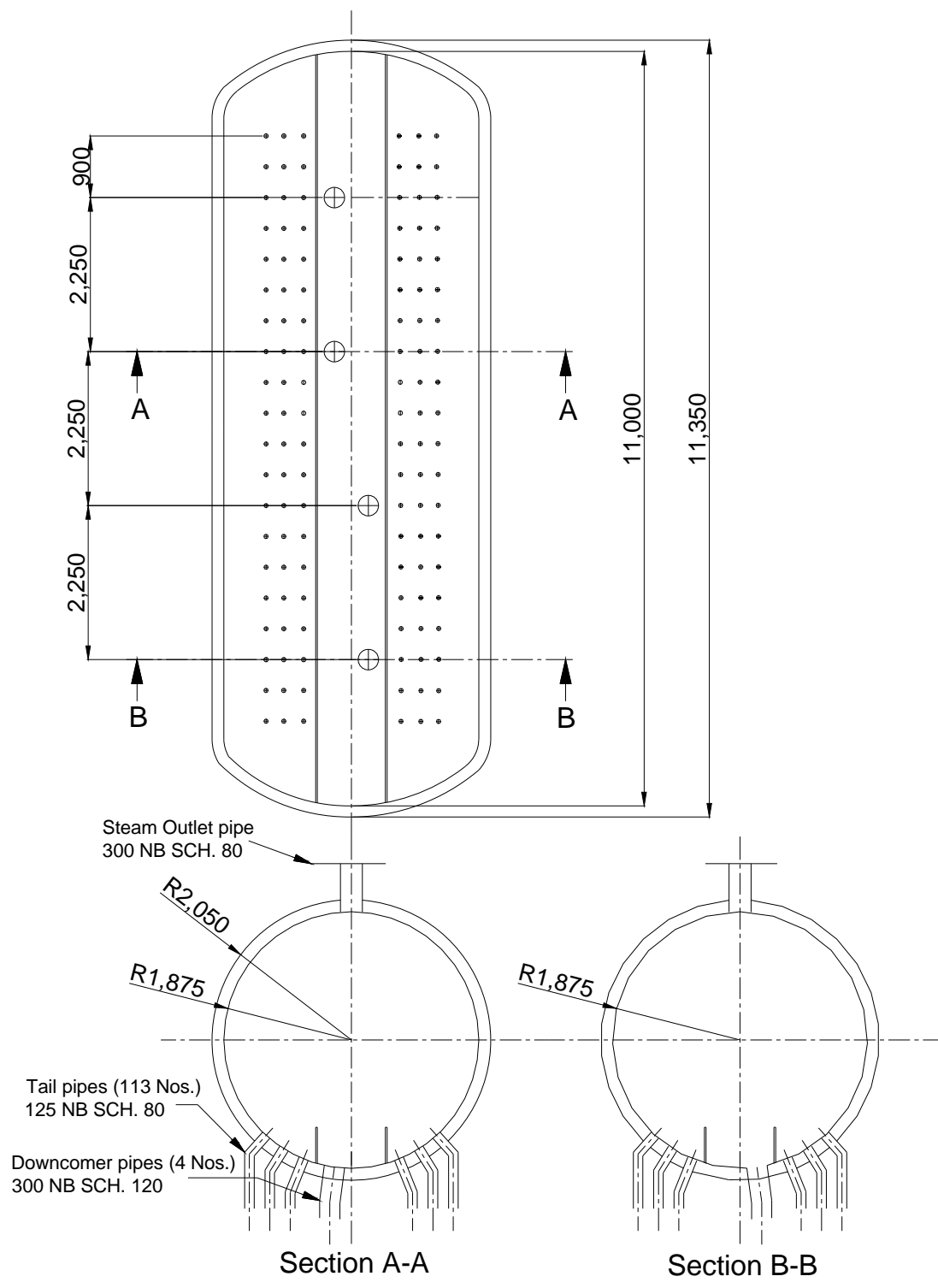


**Fig. 2a: Prototype steam drum (previous version)**

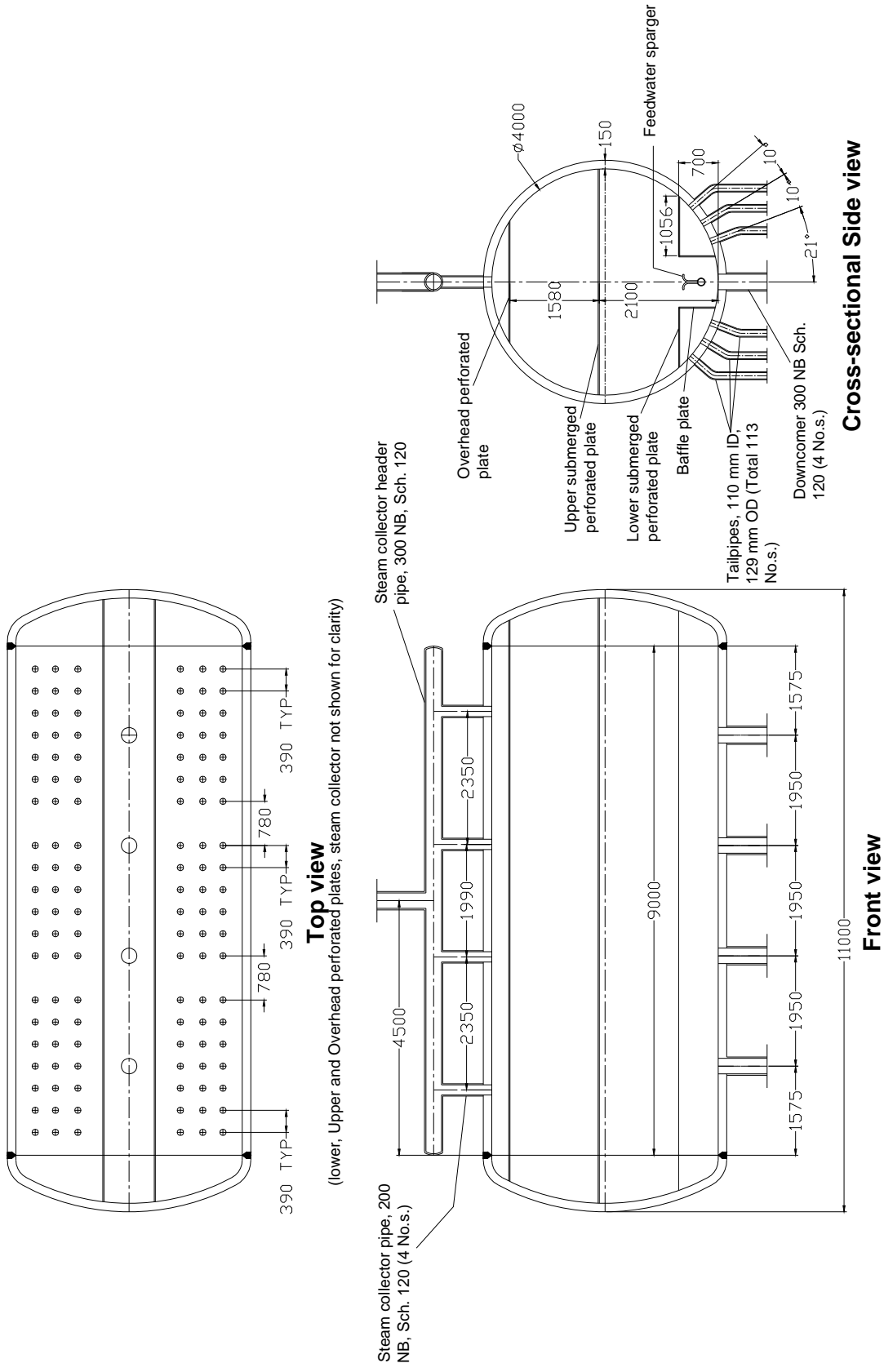


**Fig. 2b: AHWR steam drum (latest revised version)**

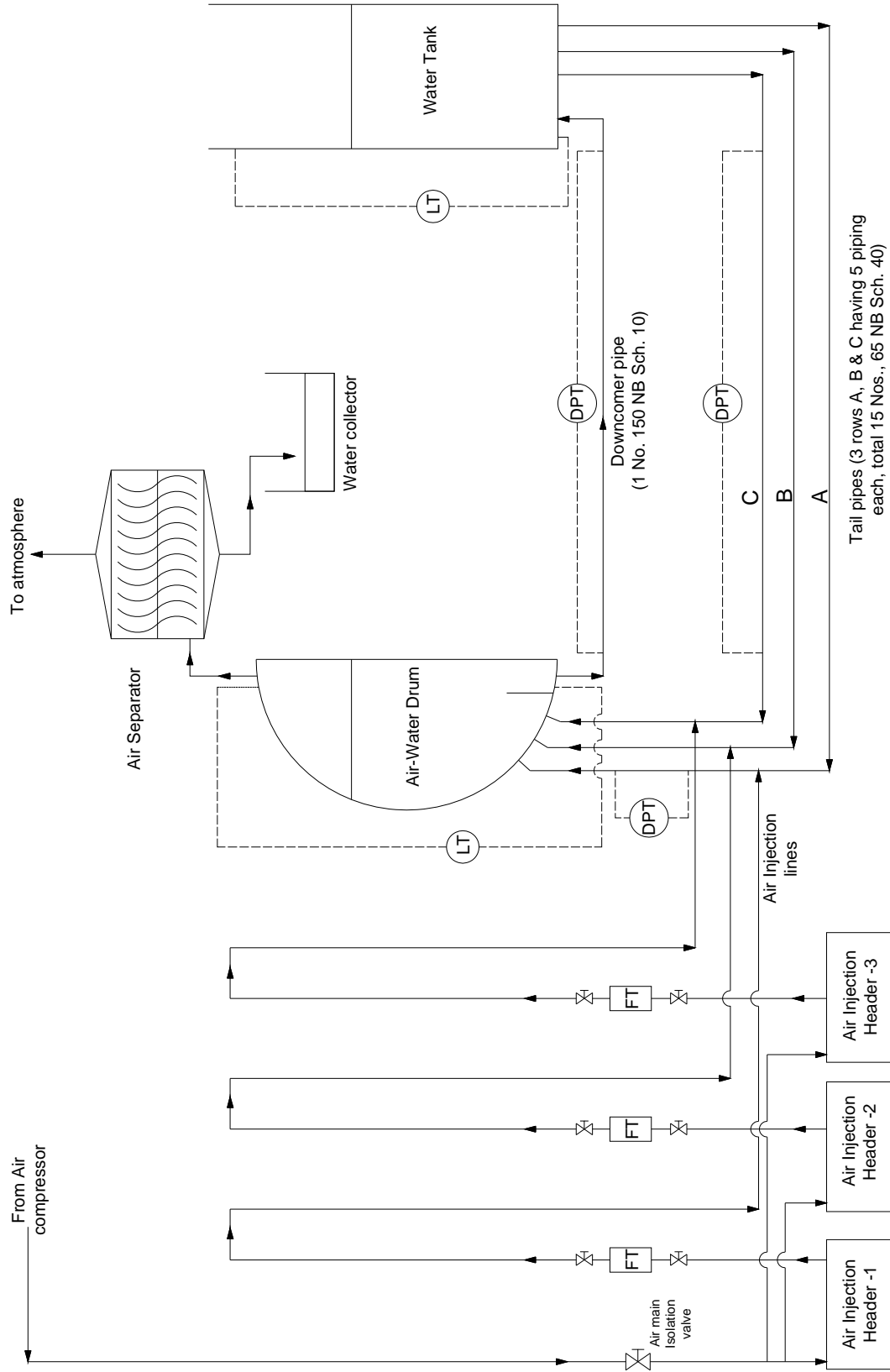


**Fig. 3: Schematic of Air Water Loop**

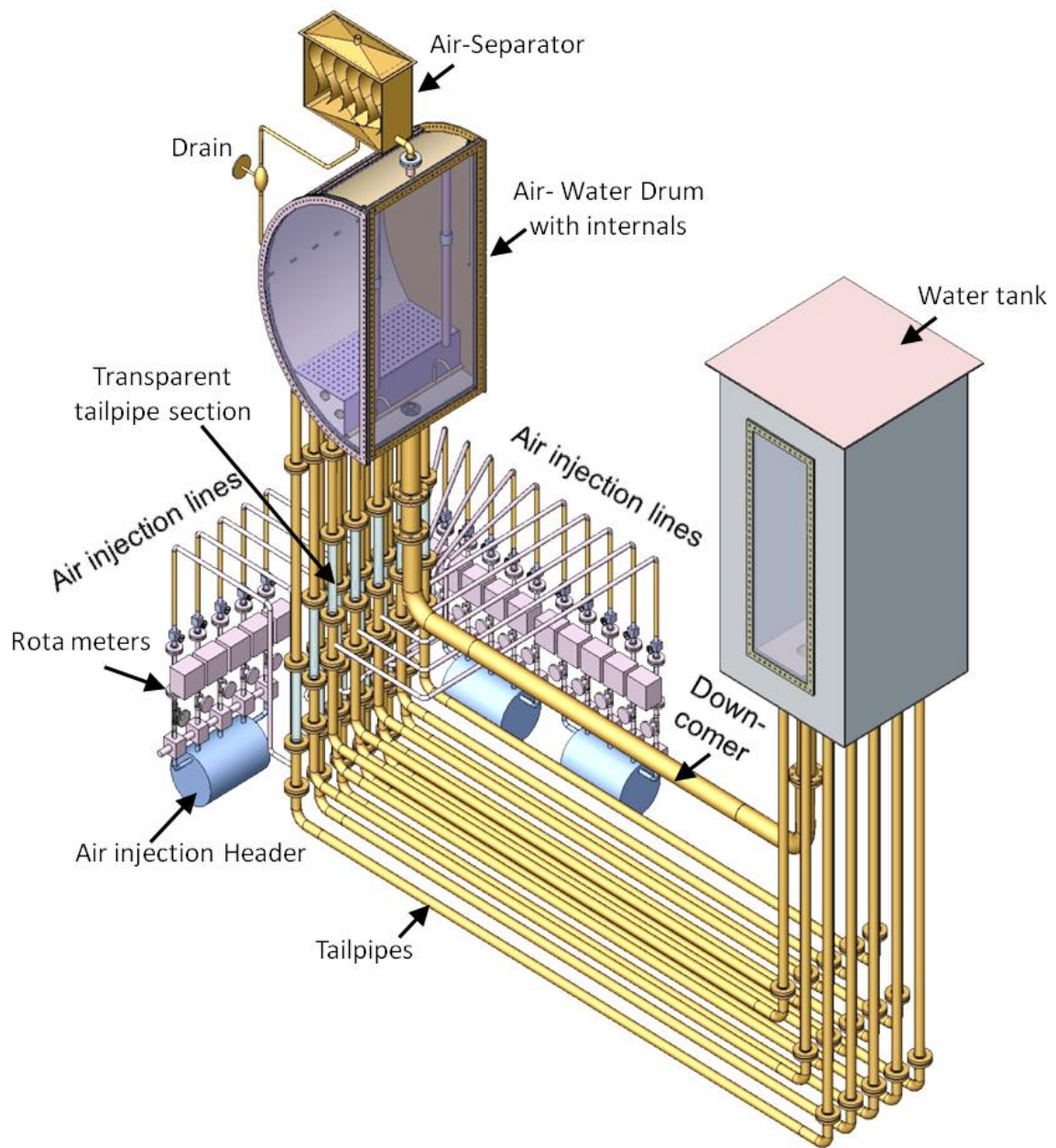


**Fig. 4: Isometric view of Air Water Loop**



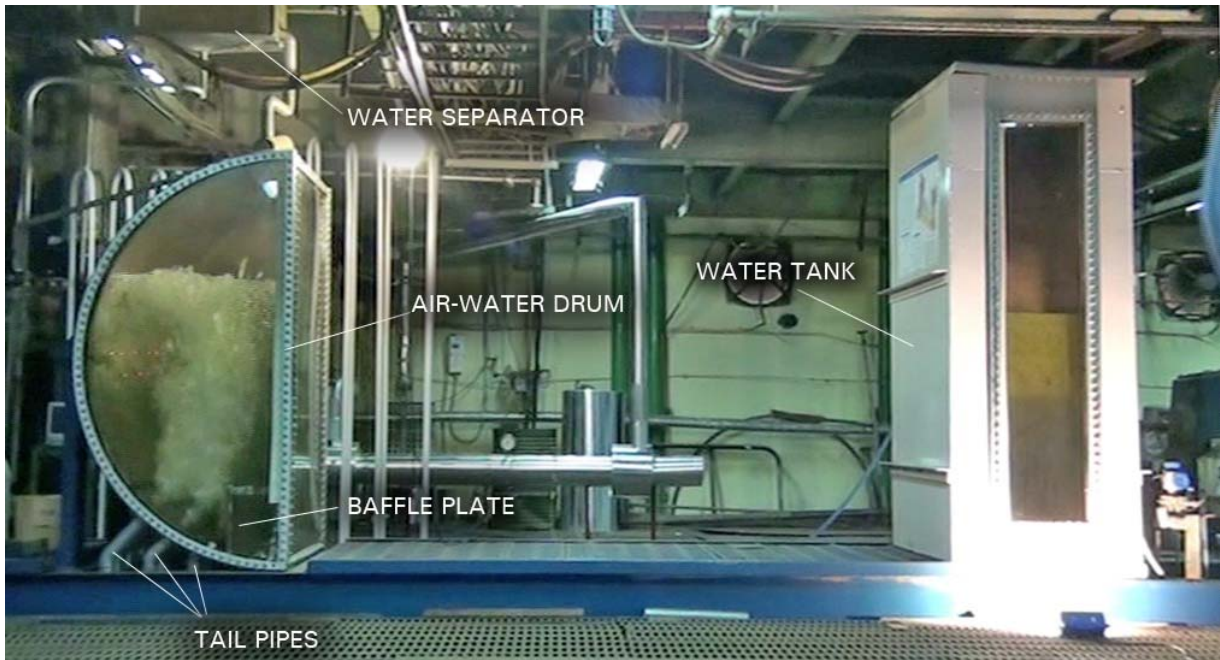


**Fig. 5: Air water drum and Water tank**



**Fig. 6: Air injection Header and Air injection lines.**

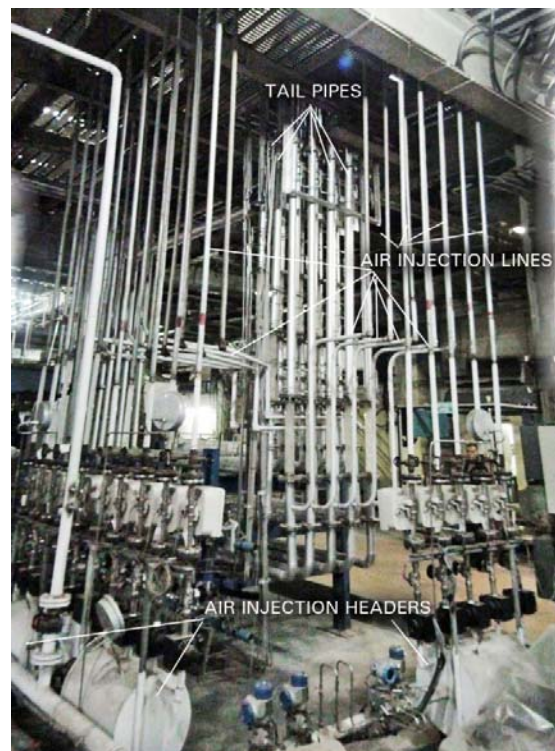


**Fig. 7: Tail pipes and Air injection lines.**

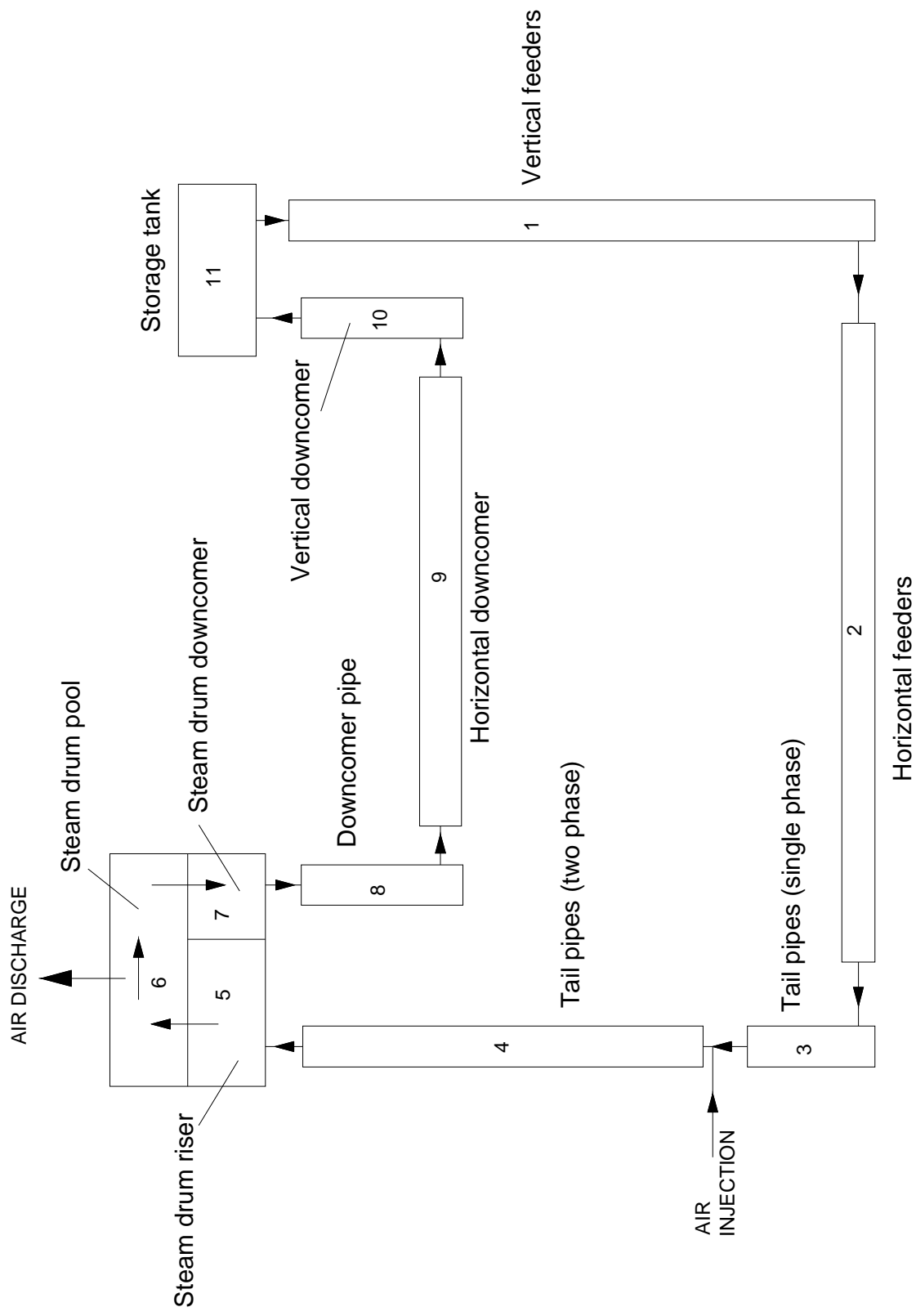


**Fig. 8: Nodalisation used for pre-test steady state flow analysis**

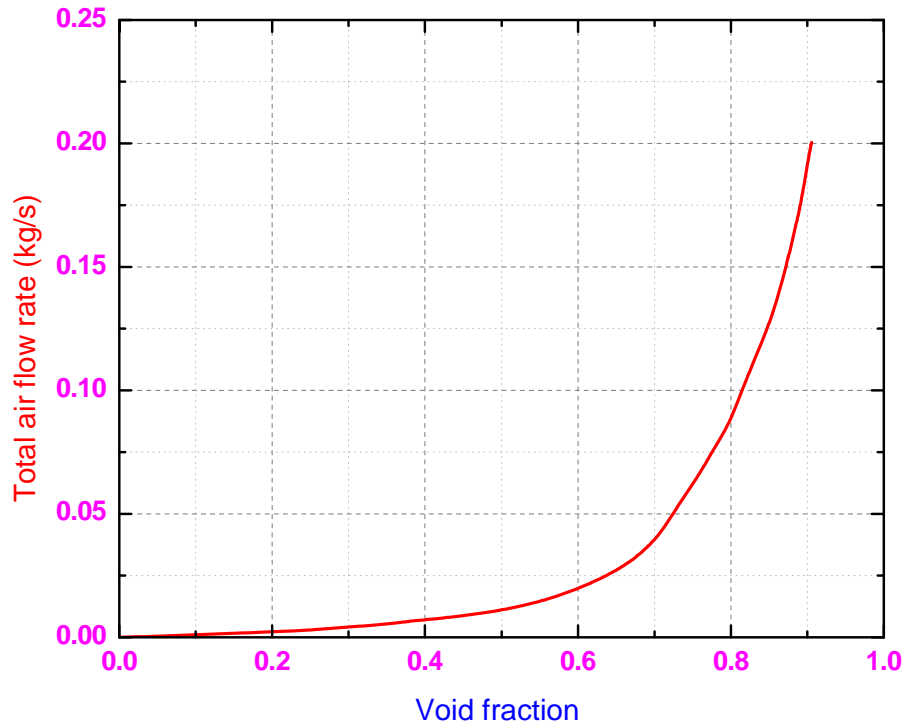


**Fig. 9: Air flow rate variation with void fraction**

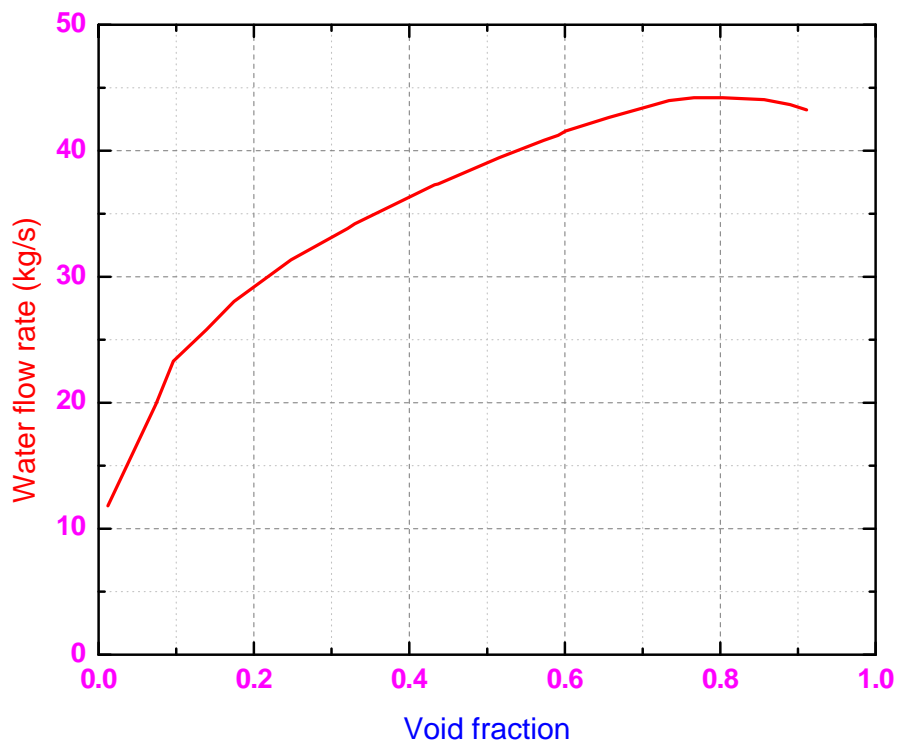


**Fig. 10: Variation of water flow rate with void fraction**

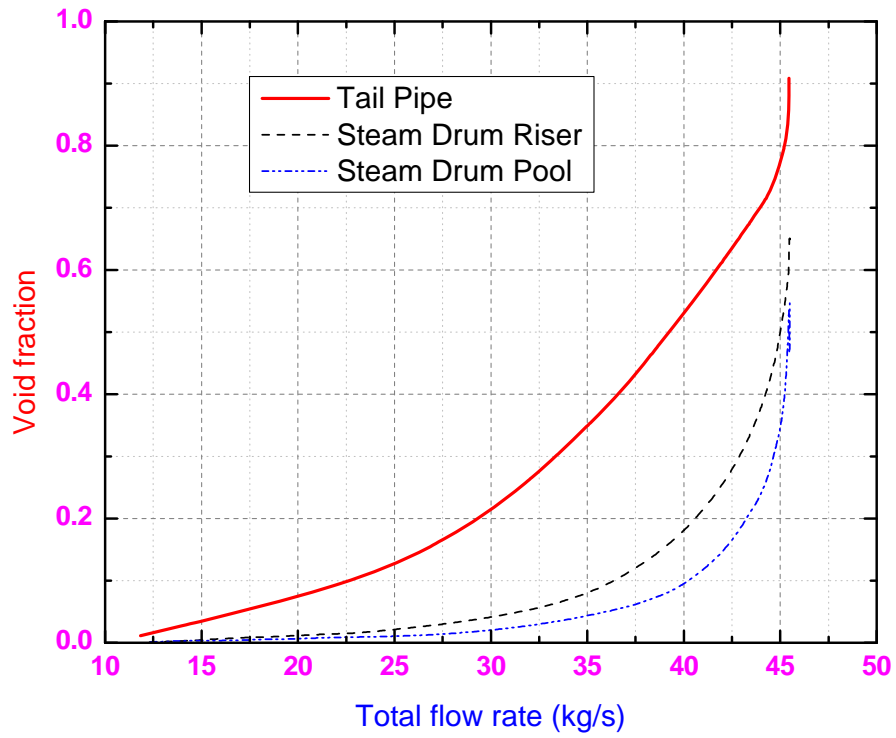


Fig. 11: Variation of void fraction in tail pipe, steam drum riser and steam drum pool

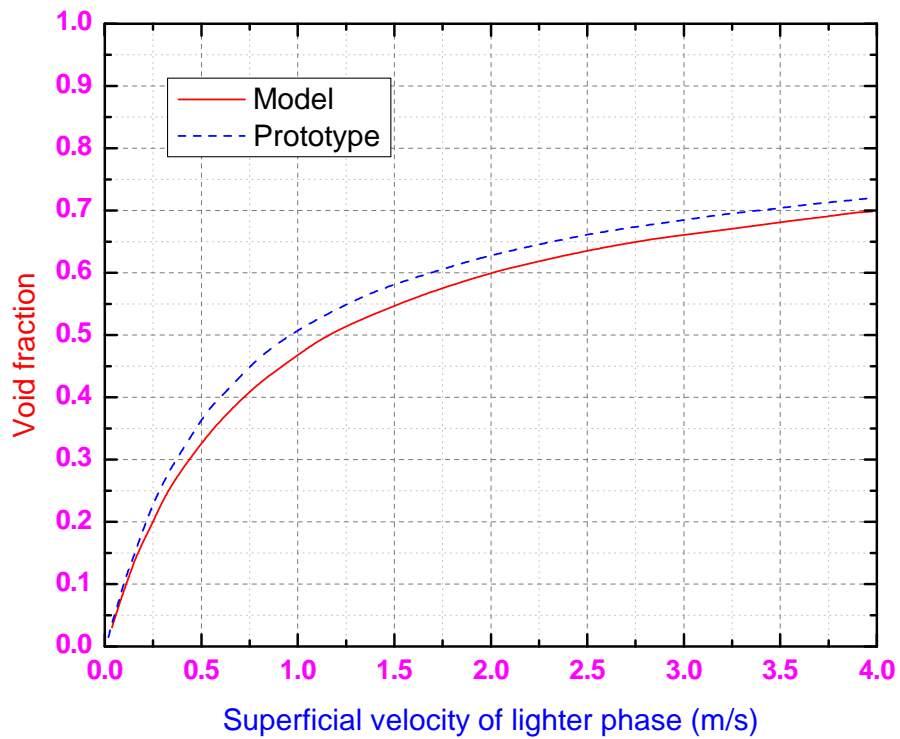
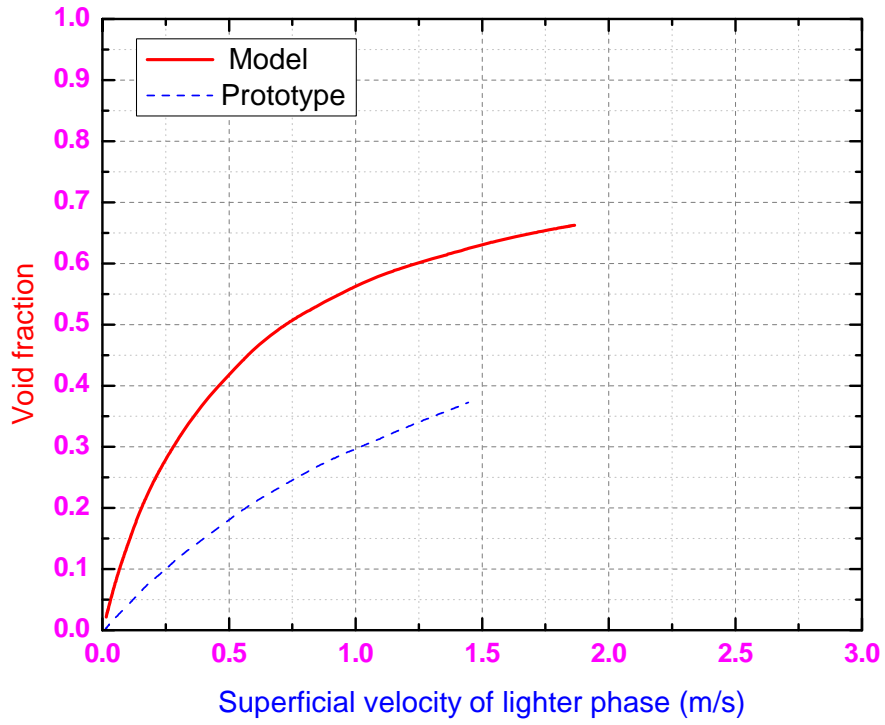
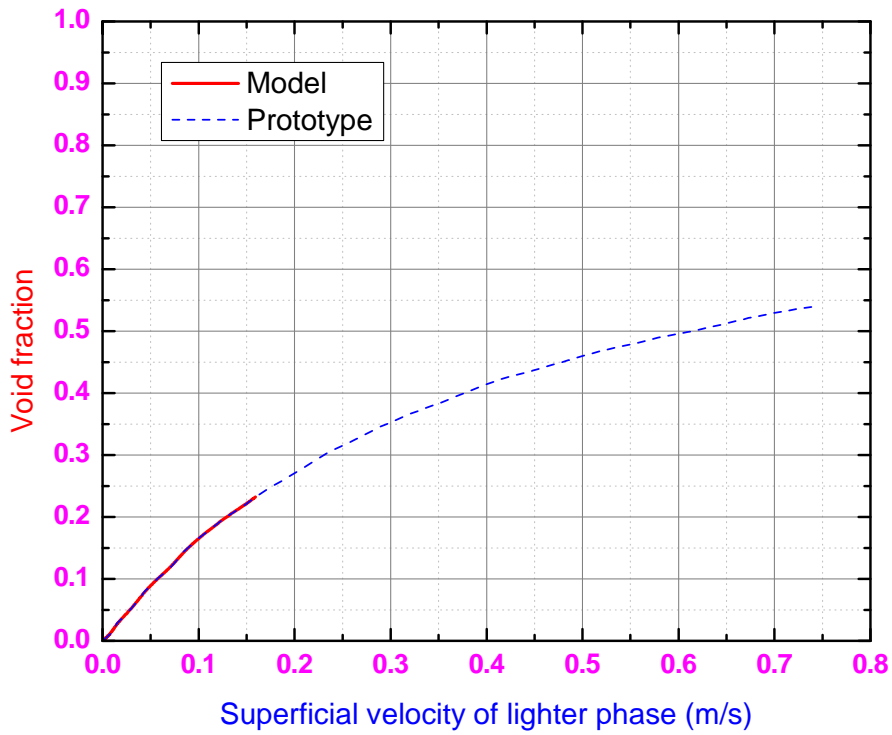


Fig. 12: Comparison of void fraction in tail pipe



**Fig. 13: Comparison of void fraction in steam drum riser**



**Fig. 14: Comparison of void fraction at steam water interface**

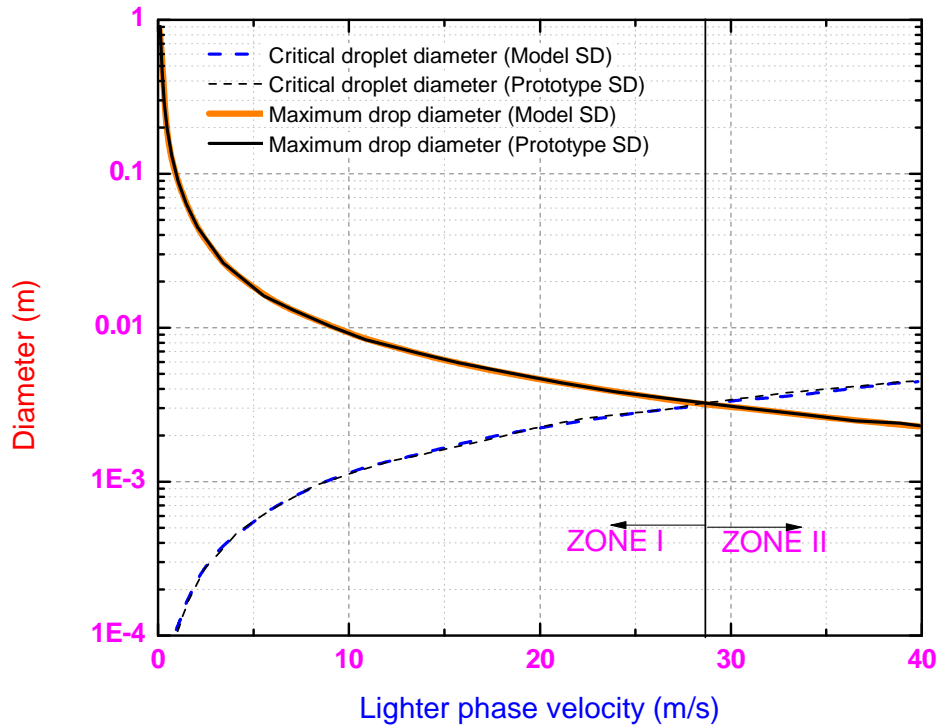


Fig. 15: Comparison of maximum droplet and critical diameter for model and prototype steam drum

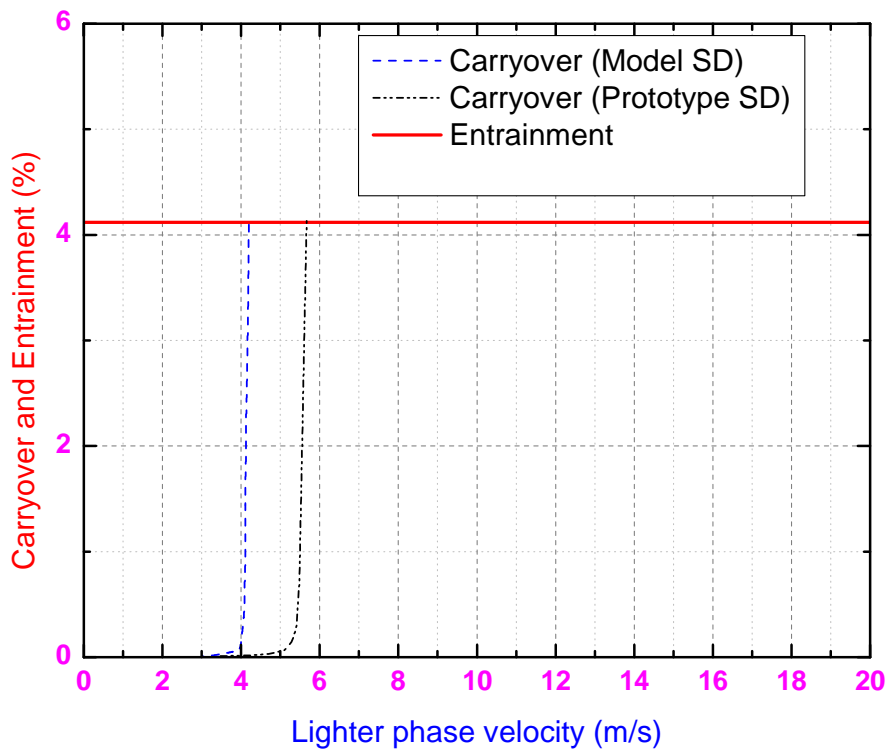
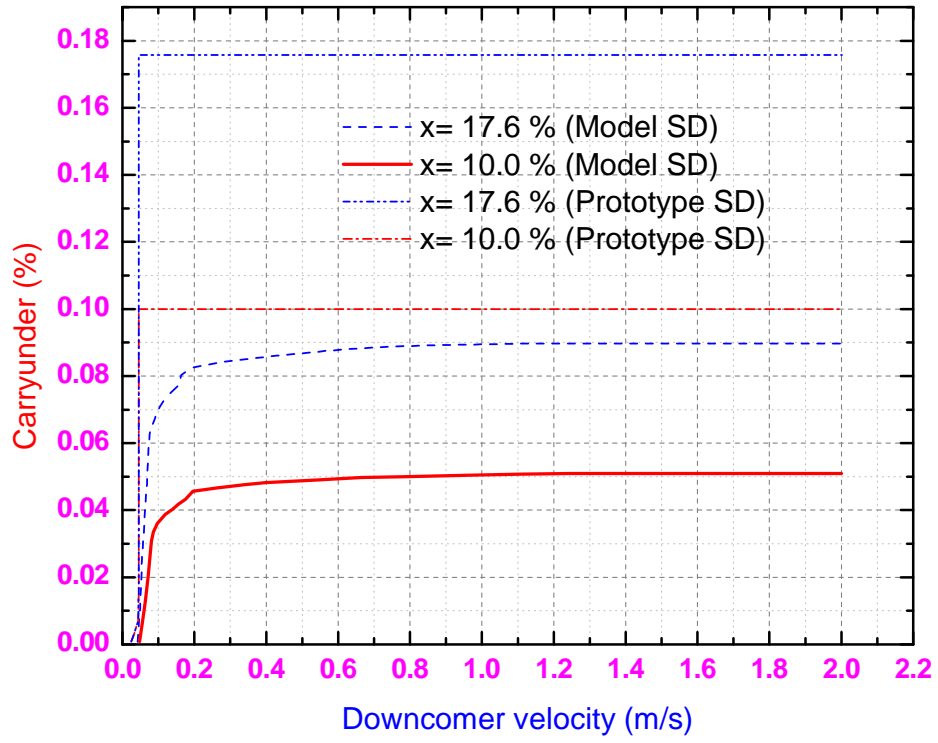


Fig. 16: Effect of air velocity on carryover for model and prototype steam drum



**Fig. 17: Effect of air velocity on carryunder for model and prototype steam drum**